Sub-specificities	Case Number	Percentage (%)	TAT (days)
Hematopath	310	24.9	7.0
Bone/soft tissue	267	21.3	5.2
GYN / Breast	259	20.7	4.3
Head/Endo/Thyroid	93	7.4	6.6
GI	89	7.1	5.2
Derm/melanoma	66	5.3	4.2
Thoracic	52	4.2	5.0
GU	48	3.8	8.5
Neuro	33	2.6	3.6
Liver	23	1.8	7.9
Pediatric	6	0.5	6.0
Others	5	0.4	6.6
Total	1251	100	5.5

Conclusions: Our results indicate that international telepathology consultation can significantly improve patient care by facilitating access to pathology expertise. The success of this international digital consultation service was dependent on strong commitment and support from leadership, information technology expertise, and dedicated pathologists. Challenges included internet speed and firewalls, difference in languages, cultures, and health care systems.

Kidney/Renal Pathology (including Transplantation)

1607 Molecular Diagnostics for Antibody-Mediated Rejection in Formalin-Fixed, Paraffin-Embedded Human Renal Allograft Biopsies

Benjamin Adam, Bahman Afzali, Nikhil Shah, Reeda Gill, Luis Hidalgo, Patricia Campbell, Michael Mengel, Banu Sis. University of Alberta, Edmonton, AB, Canada.

Background: In 2013, the Banff classification adopted molecular diagnostics (gene expression) as an adjunct for the diagnosis of antibody-mediated rejection (ABMR) in renal allografts. The new NanoString nCounter gene expression platform is unique in its ability to use samples derived from formalin-fixed paraffin-embedded (FFPE) tissue. We aimed to utilize this method to assess the validity of gene expression quantification for the diagnosis of ABMR in routine clinical FFPE renal allograft biopsies.

Design: 34 genes previously shown to be associated with ABMR were compiled into a gene set. RNA was isolated from 109 archival FFPE renal allograft biopsies. Gene set expression was quantified with the NanoString assay and correlated with clinical, serologic, and histologic data.

Results: The geometric mean of the gene set correlated with the presence of donor-specific antibodies (DSA) as well as histologic lesions of microcirculation injury and inflammation, but not tubulitis or arteritis.

Table 1: Correlation between gene set expression and serohistologic data.

Serologic/histologic feature	Correlation coefficient (r)	p-value
Donor specific antibodies (DSA)	0.51	<0.001
Glomerulitis (g)	0.41	<0.001
Transplant glomerulopathy (cg)	0.45	<0.001
Interstitial inflammation (i)	0.24	0.010
Interstitial fibrosis (ci)	0.40	<0.001
Tubulitis (t)	0.08	0.403
Tubular atrophy (ct)	0.32	<0.001
Intimal arteritis (v)	0.00	0.987
Fibrous intimal thickening (cv)	0.18	0.061
Arteriolar hyaline thickening (ah)	0.28	0.004
Mesangial matrix increase (mm)	0.44	<0.001
Peritubular capillary margination (ptc)	0.42	<0.001
Total interstitial inflammation (ti)	0.43	0.004
C4d staining (IF/IHC)	-0.09	0.387

Biopsies with a diagnosis of ABMR or mixed ABMR/T-cell mediated rejection (TCMR) had increased gene set expression compared to normal controls and DSA-negative TCMR. Interestingly, DSA-positive cases that met histologic criteria for TCMR, but not acute or chronic active ABMR, still had higher expression than DSA-negative TCMR, suggesting that some TCMR cases would be reclassified as mixed rejection when molecular diagnostics are added, as per the recent Banff 2013 recommendation.

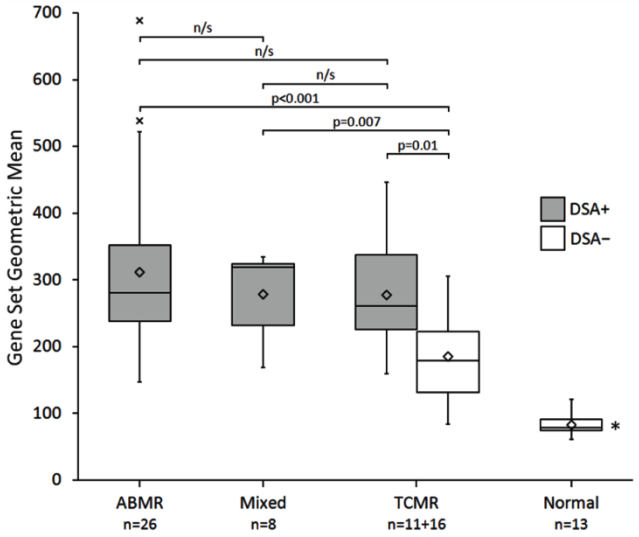

ABMR, antibody-mediated rejection; TCMR, T-cell mediated rejection; DSA, donor-specific antibody; n/s, not significant (p>0.05).
*p<0.001 for heteroscedastic two-tailed t-test between normal controls and all other diagnostic categories.

Figure 1: Gene set expression versus histologic diagnosis.

Conclusions: Our results demonstrate the feasibility of robust multiplexed gene expression quantification from FFPE renal allograft biopsies. We validated the diagnostic potential of a literature-derived ABMR gene set in routine FFPE biopsies with the NanoString platform. These data suggest a method for molecular diagnostics to be introduced into clinical transplantation pathology.

1608 Spectrum of Glomerular Disease Between the Years 2003 and 2014: Review of 11451 Cases in a Colombian Population

Luis Barrera-Herrera, Rocio Lopez, Rafael Andrade, Adriana Florez. University Hospital Fundación Santa Fe de Bogotá, Bogotá, Colombia; Universidad de los Andes, Bogotá, Colombia; Universidad Nacional de Colombia, Bogotá, Colombia.

Background: Glomerular diseases (GD) are an important cause of chronic renal failure. Prevalence of GD varies according to different socio-demographic characteristics, in Europe and North-America the most common are focal and segmental glomeruloesclerosis (FSGS) and IgA nephropathy (IGAN). Information related to GD is not very well known in Colombian patients. The aim of this study was to describe the prevalence of GD in a population from multiple areas in Colombia.

Design: Between January2003-September2014, we studied 16820 renal biopsies from multiple areas of Colombia, we excluded cases diagnosed as interstitial or tubular disease and conditions where the main damage was related with vascular injury, final sample of 11451 cases (M=5108, F=6343) age range 1 month-91 years corresponded to GD. Each case was studied with light, immunofluorescence and electron microscopy. For each biopsy information regarding age, gender, histopathological diagnosis and additional findings was available, unfortunately complete clinical information and follow up was not obtainable for most the cases. The classification of GD was based on ¨Armed Forces Institute of Pathology-2005¨ and 3 further groups of diagnostics commonly included in the hospital not included in AFIP list.

Results: From the total 11451 biopsies reported as GD, 82.3% of the cases corresponded to 5 types; first FSGS group corresponded to more frequent 22.20%(2542), the IGAN 20.13%(2305), lupus nephritis (LN) 17.30%(1981), membranous glomerulonephritis (MG) 13.06%(1496) and thin basement membrane disease (TBMD) 9,61%(1101). In relation with groups of patients under and over 18-years old (children and adults respectively), IGAN 22%(1982) was the most common in adults and FSGS 17,68%(701) in children, equally important cases included minimal change disease (MCD)17% (319), LN 15%(388), TBMD 13%(335), IGAN 13%(323) in children, and FSGS 21%(1841), NL 18%(1593), MG 15%(1350) and TBMD 9%(766) in adults.

Conclusions: This unique large cohort can serve for comparison with data from different geographic locations through the world. The information presented in this study reveals the tendency of GD in Colombian population. We confirm that FSGS is the most representative GD in children and IGAN in adults. This information will be the base to make much more specific subsequent prospective studies involving large-scale clinic-pathological correlation analysis.

1609 Dendritic Cells (DCs) in Kidney Transplant Biopsies Cluster With T Lymphocytes and Are Associated with Graft and Systemic Inflammatory Milieu and Poor Allograft Survival

Ibrahim Batal, Sacha De Serres, Maristela Onozato, Nader Najafian, Anil Chandraker. Brigham & Women's Hospital, Boston, MA; Massachusetts General Hospital, Boston, MA.

Background: Long-term renal allograft survival continues to lag behind the progress seen in short-term transplant outcomes. The negative prognostic implication of inflammation in areas of tubular atrophy (iatr) seen in kidney transplant biopsies has been increasingly recognized, however, the immunological mechanisms behind the development of such "active" atrophy have not been deciphered. DCs are the most efficient antigen-presenting cells, but surprisingly little attention has been paid to them in transplanted organs.

Design: We used DC-SIGN as a marker of DCs in allograft biopsies of 105 kidney transplant recipients. Average number of DC-SIGN$^+$ cells per high power field (hpf) was recorded. Biopsies were also stratified as having high vs. low DCs density based on the presence of more than 2 standard deviations from the mean of DC-SIGN$^+$ cell density in control nephrectomy samples. DCs were correlated with clinical and histologic variables, with immunohistochemical and FISH staining, and, in a subset of patients, with cytokine levels secreted from peripheral blood mononuclear cells (PBMCs).
Results: DCs' density was associated with poor allograft survival [HR(95% CI):1.3(1.2-1.6), P<0.01] independent of clinical variables [1.3(1.1-1.5), P= 0.006]. ROC curve showed that DC's density was capable of predicting poor outcomes in patients with high total inflammation scores (AUC: 0.7, 95% CI: 0.6-0.9, P=0.01). Graft DCs' density correlated with iatr (r=0.5, P<0.001) and with IL-1β (r=0.5, P<0.001), TNF-α (r=0.5, P=0.003), IL-6 (r=0.5, P=0.004) and MCP1 (r=0.3, P=0.03) secretion from PBMCs. Multivariate analysis indicated an independent association between the densities of T cells and DCs (P=0.02). Furthermore, ultrastructural analysis revealed direct physical contact between DCs and infiltrating lymphocytes in 12/16 (75%) of biopsies with high DCs density that had material available for ultrastructural evaluation. To understand the dynamics of this process, the origin of graft DCs was assessed in 9 sex-mismatched recipients using XY FISH. Whereas donor DCs predominated initially, the majority of DCs in late allograft biopsies were of recipient origin.
Conclusions: Our data highlight the importance of assessing DC-SIGN$^+$ cells in allograft biopsies, suggest a new role for DCs in shaping alloinflammation likely by stimulating an *in situ* immune response, and provide a rationale for targeting DCs' recruitment to improve long-term allograft survival.

1610 The Phenotypic and Functional Characteristics of Dendritic Cells (DCs) Resident in the Kidney (kDCs)

Ibrahim Batal, Jan Herter, Jamil Azzi, Andrew Lichtman, Tanya Mayadas. Brigham & Women's Hospital and Harvard Medical School, Boston, MA.

Background: kDCs are abundant renal leukocytes that have traditionally been labeled as macrophages (MΦ). To study the functional roles of kDCs, investigators have heavily relied on systemic depletion of DCs, which (1) does not differentiate kDCs from DCs recruited to the kidney during injury and (2) might potentially be misleading due to depletion of extrarenal DCs. In the transplant setting, we showed that graft DCs that cluster with infiltrating T cells were mainly recruited to the kidney from the recipient. Hence, the role of resident kDCs in promoting or regulating renal inflammation remains largely unknown.
Design: We characterized kDCs with regard to 4 important DC features: microanatomy, cytokine profile, migration, and T cell stimulation. The distribution of kDCs was studied in CX3CR1^{GFP+} mice using nonfiltered and filtered fluorescent-labeled dextran. Pure viable kDCs were isolated by CD11c immunomagnetic beads from C57BL/6 mice and characterized in comparison to splenic DCs (SDCs). Morphology was assessed by electron microscopy, cytokine secretion in the supernatant of DCs incubated overnight with GM-CSF was studied by Luminex, and CFSE-labeled DCs migration from the footpad to the popliteal lymph nodes of BALB/c mice was assessed by flow cytometry (FC). Finally, DCs were incubated with CFSE-labeled BALB/c CD8$^+$ or CD4$^+$ T cells where T cell proliferation and cytokine secretion were assessed by FC and Luminex, respectively. All experiments were performed under steady state conditions.
Results: Occasional kDCs revealed intimate association with vascular lumen suggesting a possible contact with peripheral blood through the peritubular capillaries. Compared to SDCs, kDCs were smaller in size (P<0.001), had higher percentage of CX3CR1$^+$F4/80$^+$ MΦ-like cells (P=0.03), and showed inferior migration (P=0.04). Still, kDCs had lower expression of programmed cell death 1 ligand (PD-L1) (P=0.046), and secreted higher levels of IL-6 (P=0.02) and IP-10 (P<0.001). kDCs had decreased cytotoxic T cell proliferation (P=0.02) accompanied by >10 folds decrease in IL-2 secretion. Although kDCs showed decreased helper T cell proliferation (P=0.02), they tended to have lower Tregs generation capability (P=0.1).
Conclusions: kDCs have a hybrid phenotype between DCs and MΦ. Although kDCs have suboptimal T cell stimulation and migration, their cytokine profile, low PD-L1, and inferior Tregs generation suggest a potential role in promoting renal inflammation. How these kDCs characteristics are altered following stimulation is an issue that remains to be addressed.

1611 Podocyte-Specific Myh9 Deletion in Mice Results in Susceptibility To Glomerular Injury in Response To Subtotal Nephrectomy

Mostafa Belghasem, Mei Cao, Philip Bondzie, Joel Henderson. Boston University, Boston, MA.

Background: The gene MYH9 encodes non-muscle myosin IIA, an essential podocyte contractile protein. The increased incidence of chronic kidney disease in African Americans has been linked to genetic variation near MYH9, and rare hereditary syndromes involving mutations in MYH9 often include renal involvement. The genetic features of these forms of MYH9-associated kidney disease suggest that altered MYH9 expression levels could play a role in disease pathogenesis. The objective of this study is to determine the effect of MYH9 ablation on non-muscle myosin expression and kidney structure, and response to hemodynamic stress, using podocyte-specific Myh9 knockout mice.
Design: We investigated the role of Myh9 in renal injury after subtotal nephrectomy. Podocyte-specific Myh9 knockout mice on a C57BL/6 background and controls were subjected to subtotal 5/6 nephrectomy for 8 weeks. During treatment, systemic blood pressure was measured by the tail cuff method, and kidney function was assessed with urine and serum biomarkers. At the end of the treatment period, kidney tissue was collected and kidney morphology was evaluated by light and electron microscopy.
Results: Myh9 knockout mice showed glomerular hypertrophy, podocyte foot effacement, glomerular basement membrane thickening and exacerbation of urinary albumin excretion, after subtotal nephrectomy compared with control mice. In addition, the knockout mice showed persistent elevation of systolic blood pressure.
Conclusions: Podocyte-specific Myh9 ablation renders mice susceptible to glomerular injury when subjected to 5/6 nephrectomy. This suggests that non-muscle myosin IIA plays an important role in protecting the glomerulus from hemodynamic stress indcuded by subtotal nephrectomy. Nevertheless, under normal physiological conditions podocyte-specific Myh9 ablation had no significant effect on kidney structure and function.

1612 Tubular Basement Membrane Thickness in Thin Basement Membrane Disease

Mei Lin Bissonnette, Kammi Henriksen, Anthony Chang. University of Chicago, Chicago, IL.

Background: Thin basement membrane disease (TBMD) is an inherited glomerular disorder characterized by persistent microscopic hematuria and few pathologic abnormalities other than thin glomerular basement membranes (GBMs). On occasion, glomeruli may not be available in the sample for electron microscopy, which would require another biopsy to establish the diagnosis. Up to 40% of TBMD cases have COL4A3 and COL4A4 mutations in collagen IV, and the a3, α4, and α5 chains of collagen IV are expressed in distal tubular basement membranes as well as GBMs. We conducted this study to determine whether measurement of tubular basement membranes could be useful in the diagnosis of TBMD.
Design: GBM, proximal tubular basement membranes (PTBM), and non-proximal tubular basement membranes (NPTBM) were measured by electron microscopy in human kidney biopsies with TBMD (n=4) and MCD (n=4). For all cases, no other disease processes were present. Areas of tubular atrophy, if present, were avoided. For each case, multiple peripheral capillaries from 1-2 glomeruli, 10 proximal tubules, and 4-10 non-proximal tubules were measured, based on sample size. Fifty measurements were averaged in each category per case.
Results: The basement membrane measurements for the 4 cases of TBMD and 4 cases of MCD are summarized in Table 1. The average GBM thickness was 205 nm (TBMD) and 368 nm (MCD), p-value<0.01. The average PTBM thickness was 392 nm (TBMD) and 502 nm (MCD), p-value=0.12. The average NPTBM thickness was 290 nm (TBMD) and 518 nm (MCD), p-value<0.05.

Case #	Age/Sex	GBM (nm)	PTBM (nm)	NPTBM (nm)
TBMD 1	48/M	203 (119-269)	507 (293-701)	314 (182-562)
TBMD 2	41/F	205 (139-293)	430 (159-770)	347 (150-707)
TBMD 3	39/M	210 (140-288)	327 (196-602)	290 (106-1090)
TBMD 4	64/F	203 (101-293)	305 (176-602)	210 (106-469)
MCD 1	51/M	412 (290-581)	584 (288-842)	306 (165-806)
MCD 2	40/F	313 (197-438)	424 (252-875)	545 (314-1070)
MCD 3	32/M	380 (291-610)	434 (232-806)	563 (221-1030)
MCD 4	64/F	370 (223-448)	564 (356-879)	657 (288-1210)

Conclusions: In TBMD, the NPTBM and, to a lesser extent, the PTBM are also thin in addition to the GBM. This suggests tubular measurements, especially NPTBM, may be useful in the diagnosis of TBMD. Further studies are needed to determine whether this could be a surrogate parameter to establish the diagnosis of TBMD.

1613 Nephropathy in the Setting of Substance Abuse: An Analysis of 153 Medicolegal Deaths

Melissa Blessing, R Ross Reichard, Joseph J Maleszewski, Ross Dierkhising, Loralie Langman, Mariam Priya Alexander. Mayo Clinic, Rochester, MN.

Background: Substance abuse is an escalating public health problem, accounting for increased numbers of unnatural deaths. The kidney, which excretes most of these drugs or their metabolites, is frequently injured; however, to date, systematic reviews of the spectrum of renal pathology in the setting of drug abuse are limited.
Design: Tissue registry archival databases of Mayo Clinic (Rochester, MN) were queried for cases with a history of substance abuse and positive postmortem (PM) toxicology (2011-2013). Renal slides were reviewed by a renal pathologist in a blinded fashion and histopathological changes of the kidney were noted. Salient clinical history, other organ pathology, and PM toxicology was recorded. Logistic regression was used to measure associations with renal histology. Multivariable models were obtained using forward variable selection with subsequent backwards elimination.
Results: 153 cases (mean age 45 yrs., range 15-79; 67% men) were evaluated. Death due to acute drug/toxin toxicity accounted for 51% of deaths. Chronic alcohol abuse was the second most common cause of death (10%). PM toxicology was most commonly positive for alcohol (38%) followed by opiates (24%). The spectrum of renal histopathology included arteriolosclerosis (71%), mesangial sclerosis (50%), acute tubular injury (73%), cortical congestion (15%) and medullary congestion (20%). Crystals, predominantly calcium phosphate, were seen in 20% of our cases. Common co-morbidities included coronary artery disease (52%) and hypertension (36%). In multivariate analysis, tubulointerstitial pathology was the most frequent renal abnormality. Specifically, both marijuana and acetaminophen use had odds ratios of infinity and p=0.001. Glomerular pathology was associated with a history of alcohol abuse (odds ratio 0.338; p=0.10) and vascular changes with benzodiazepines (odds ratio 4.5; p=0.04).

Conclusions: A broad but non-specific spectrum of renal pathology is seen in association with substance abuse. Tubular damage noted with acetaminophen use may be mediated by cytochrome P450. Marijuana-related tubular injury has been previously described, and raises concern in the age of medical marijuana. The vascular changes seen with benzodiazepine exposure were novel, and warrant further study. The association of alcohol and glomerulopathy has not been well-described in literature. Future investigation into the pathogenesis of drug-related toxicity is critical to developing prevention and treatment strategies.

1614 The Distinctive Eosinophilic Cysts of Tuberous Sclerosis Complex Are Derived From Proximal Tubules

Christie Boils, Ping Zhang, Neriman Gokden, David Grignon, Xin Gu, Samih Nasr, Carrie Phillips, Stephen Bonsib. Nephropath, Little Rock, AR; William Beaumont Hospital, Royal Oak, MI; University of Arkansas, Little Rock, AR; Indiana University, Indianapolis, IN; Louisiana State University, Shreveport, LA; Mayo Clinic, Rochester, MN.

Background: Tuberous sclerosis complex (TSC) is due to mutation of *TSC1* or *TSC2*, genes whose protein products, hamartin and tuberin, inhibit the mammalian target of rapamycin (mTOR) pathway. TSC is associated with a variety of renal lesions, cysts and polycystic kidney disease (PKD), and neoplasms. The cysts may be lined by a flat attenuated or low cuboidal epithelium (F/C-cysts) or by distinctive epithelium composed of large eosinophilic cells (E-cysts) regarded as characteristic of TSC. This study examines the tubular segment origin of the eosinophilic cysts and presence of mTOR activation in cysts.

Design: Nine cases of TSC were studied, 9 complete and 3 partial nephrectomies for a total of 12 specimens. Four cases contain E-cysts and angiomyolipomas. Five cases contained diffuse E-cysts and F/C-cysts of PKD. Cyst epithelium was analyzed using immunoperoxidase stains for CD10, cytokeratin 7 (CK7), kidney injury molecule-1 (KIM-1), p-mTOR and p-p70S6K (a downstream signal of mTOR activation).

Results: The majority of E-cysts were CD10 positive and CK7 negative (Table 1), consistent with a proximal tubule (PT) phenotype. Conversely, the majority of F/C-cysts were CD10 negative and CK7 positive consistent with a distal tubule (DT)/collecting duct (CD) phenotype. KIM-1 staining showed that 50% of E-cysts and 31% of F/C-cysts were positive. Markers of mTOR activation show 1+ to 2+ staining in the F/C-cystic epithelial cytoplasm and nuclei, similar to expression of DT/CD.

	CD10	KIM-1	CK7
# Cases	# E-Cysts Positive / Total # E-Cysts		
9	46/47	25/50	2/39
	# F/C-Cysts Positive / Total # F/C-Cysts		
9	3/19	5/16	26/27

Conclusions: 1) The cyst lining in TSC is heterogeneous, ranging from flat or low cuboidal, to large eosinophilic cells. 2) Immunoperoxidase stains support PT differentiation of E-cysts and DT/CD differentiation of F/C-cysts. 3) Markers of mTOR activation are present along F/C-cyst walls, compatible with contribution of upregulated mTOR pathway in cyst proliferation.

1615 Renal Biopsy Findings and PLA2R Status in Pregnancy-Associated Membranous Nephropathy

Lihong Bu, Jolanta Kowalewska, Christine VanBeek. Cedars-Sinai Medical Center, Los Angeles, CA.

Background: There are only rare reports of membranous nephropathy (MN) with initial onset during pregnancy in patients without evident underlying systemic disorders. Our aim is to describe the clinicopathologic features including PLA2R status in a series of patients with pregnancy-associated MN.

Design: We searched the pathology database to identify native renal biopsies obtained from pregnant or post-partum females with MN who initially developed proteinuria during pregnancy. Standard light microscopy (LM), immunofluorescence (IF), and electron microscopy (EM) were examined in all cases. Additionally, PLA2R immunohistochemistry was performed on formalin-fixed paraffin embedded tissue in 10 cases with adequate tissue and IgG subclass analysis was done by IF in all cases. Available clinical information was reviewed.

Results: Of 18,612 native renal biopsies examined from 2007-2014, 11 biopsies with pregnancy-associated MN were identified. All patients (age range of 19 - 39) had nephrotic-range proteinuria which initially manifested during pregnancy, commonly during the second or third trimester. None of the patients had pre-existing renal disease or other known comorbidities. Serologic studies were largely negative, except in two patients who had a positive ANA without other symptoms of systemic lupus. By LM, mesangial hypercellularity was noted in one case, while glomeruli in remaining cases were normocellular. Crescents, necrosis, and endocapillary hypercellularity were not seen in any case. By IF, granular capillary wall staining was noted for IgG and C3, without significant staining for other immunoglobulins or C1q. Ultrastructurally, in addition to subepithelial deposits, a subset of patients also had subendothelial deposits (n=2), mesangial deposits (n=6), and tubulo-reticular inclusions (n=2). PLA2R was negative in subepithelial deposits in all 10 tested cases. IgG subclass analysis revealed IgG1 dominant staining in 7 (64%) cases and co-dominant staining for IgG1 and IgG4 in the remaining 4 (36%) cases.

Conclusions: Pregnancy-associated MN is PLA2R negative and usually has an IgG1 dominant or IgG1 and IgG4 co-dominant pattern. The underlying trigger of this disease appears to be the pregnancy itself, but the target antigen is not yet known.

1616 Monoclonal Immunoglobulin Deposition Disease (MIDD) Without Glomerular Proteinuria

Mongkon Charoenpitakchai, Paisit Paueksakon. Vanderbilt University Medical Center, Nashville, TN.

Background: Renal monoclonal immunoglobulin deposition disease (MIDD) is characterized by nodular sclerosing glomerulopathy, proteinuria, renal insufficiency, and an association with dysproteinemias. There are 3 subtypes of MIDD, including LCDD, LHCDD and HCDD. Only 16% of patients with LCDD were previously reported in the literature to have <1 g/day proteinuria but clinical and pathological characteristics of this entity remain poorly described.

Design: Twenty-eight patients with MIDD in our 2004-2014 renal biopsy files at VUMC were reviewed. There were 22 patients with LCDD, 4 patients with LHCDD and 2 patients with HCDD. A semi-quantitative index G score (0-4) was used to evaluate the degree of glomerular mesangial expansion and sclerosis by LM. IF and EM were analyzed as presence or absence of monoclonal protein deposits. Clinical data of these patients were reviewed.

Results: Twenty-two patients with LCDD, ranged from 46 to 81years old (mean 63.2±10.4) and male/female ratio 1/1.2. All 4 patients with LHCDD and 2 patients with HCDD are male, ranged from 54 to 60 years old (mean 56.3±2.6) and 46 to 63 years old (mean 54.5±12.0), respectively. Seven of 22 patients with LCDD had <1.0 g/day proteinuria at the time of diagnosis while all LHCDD and HCDD patients had >1.0 g/day proteinuria. Patients with LCDD were defined in 2 groups: group 1 <1.0 g/day proteinuria and group 2 ³1.0 g/day proteinuria. Mean G score of group 1 was 1.0 ($p < 0.05$ vs. group 2). One patient (14.2%) in group 1 had only tubular deposition without glomerular deposition while all patients in group 2 had both glomerular and tubular deposition by IF and EM.

Conclusions: About one third of LCDD patients had low grade proteinuria <1.0 g/day while all patients with LHCDD and HCDD had > 1.0 g/day. Group 1 LCDD patients had less nodular sclerosis than group 2. The dyssynchronous tubular basement membrane deposits versus glomerular basement membrane deposits in some of LCDD cases suggested that LCDD may in a subset of patients be preferentially tubulopathic and thus manifest no or minimal glomerular proteinuria.

1617 Correlation of Donor Specific Antibody (DSA) Class and Amount With Morphological Features of Antibody Mediated Rejection (AMR) in Renal Transplant Biopsies: Importance of Cellular Elements and DSA Type

Muhammad Reza Chaudhry, Abdolreza Haririan, Cinthia Drachenberg, John Papadimitriou. University of Maryland School of Medicine, Baltimore, MD.

Background: AMR is a complex process of allograft destruction affecting the microvasculature. The process involves the DSA, complement, inflammatory cell components (including CD68+ macrophages and CD3+ lymphocytes), endothelial cells (as primary targets), and secondarily podocytes. The individual significance of these components in the evolution of AMR is not completely understood.

Design: We selected 388 consecutive biopsies from 272 patients that had electron microscopic (EM) studies and concurrent DSA positive studies. Each case was scored for glomerulitis (g), capillaritis (ptc), transplant glomerulopathy (cg), maximum glomerular CD68 and CD3 counts, C4d staining; and on EM for the degree of endothelial swelling, podocyte foot process (FP) effacement, and number of layers in peritubular capillary lamellations (PTCML) and presence or absence of subendothelial expansion/basement membrane duplication. These parameters were correlated with each other and with total DSA MFI (mean fluorescence index), HLA Class I and II MFI, as well time post-transplant.

Results: The vast majority (g,cg,CD68,CD3,C4d,endothelial swelling,PTCML, podocyte FP effacement) of the parameters of glomerular inflammation/ microvascular injury correlated significantly with each other [r=.74-.12; p=.02-.0000]. Biopsy post-transplant time correlated mainly with g, cg, and podocyte effacement (p=.024; p=.0002; p=.0270 respectively). Numbers of antibodies of all DSA (p=.0000) and individually both of Class I and II DSA correlated statistically with endothelial swelling (p=.02 and p=.0001, respectively), but only the MFI of Class II was significant (p=.0000). Similarly, the subendothelial expansion/duplication and podocyte injury correlated significantly with number of antibodies and MFI of DSA Class II only (p=.000, p=.01, respectively).

Conclusions: AMR is a complex interplay of DSA, complement, inflammatory cells and endothelial cells that evolves over time affecting secondarily other renal elements (e.g. podocytes). These results strengthen the concept that the cellular inflammatory components (primarily macrophages and secondarily lymphocytes) play a central role in the microvasculature destruction, since their numbers correlate significantly with the degree of microvascular changes. DSA Class II antibodies appear to be at least quantitatively more important in the endothelial/microvascular chronic glomerular injury.

1618 Dendritic Cells in Renal Biopsies of Patients With Acute Tubulointerstitial Nephritis

Mingyu Cheng, Guillermo Herrera. Louisiana State University Health Sciences Center, Shreveport, LA.

Background: Dendritic cells (DCs) play a critical role in the regulation of the adaptive immune response and can be separated into two major subsets: myeloid and plasmacytoid DCs. Their involvement in acute tubulointerstitial nephritis (ATIN) is unknown. In this study, the participation and localization of DC subsets were investigated in ATIN.

Design: A total of 29 renal biopsies from patients with ATIN (n=12), lupus nephritis (n=10, positive controls), or minimal change disease (MCD, n=7, negative controls) were studied. All biopsies were investigated with direct immunofluorescence (DIF) for myeloid (CD1c) and plasmacytoid (CD303) renal DC subsets. The amount of DCs

in the biopsies was determined by area measurement using the digital image analysis system ImageJ. Positively stained area was expressed as a fraction of the area of the high power field examined. The ultrastructural features of DCs in renal biopsies were evaluated by transmission electron microscopy (TEM). All numerical data were expressed as mean ± standard error (SEM) and analyzed using one-way ANOVA in conjunction with Tukey's *post hoc* test.

Results: DCs were identified morphologically within the tubulointerstitium in the renal biopsies by TEM interacting with surrounding tubules and inflammatory cells. DIF staining showed few CD1c positive cells and CD303 positive cells in the biopsies with MCD. As compared with MCD, biopsies with ATIN had significantly increased CD1c positive cells (4.81% ± 0.37% vs 0.91% ± 0.31%, $p<0.001$) and CD303 positive cells (3.61% ± 0.4% vs 0.59% ± 0.26%, $p<0.001$). The number of CD1c positive cells in ATIN were significantly higher than that in lupus nephritis (4.81% ± 0.37% vs 3.15% ± 0.45%, $p<0.02$), whereas the number of CD303 positive cells in ATIN was slightly but not significantly higher than that in lupus nephritis (3.61% ± 0.4% vs 2.75% ± 0.47%, $p=0.2$). CD1c and CD303 positive cells in biopsies with ATIN and lupus nephritis were exclusively restricted to the tubulointerstitium.

Conclusions: Both myeloid and plasmacytoid DCs are significantly increased in the tubulointerstitium in ATIN as compared to those in MCD, suggesting these two subsets of DCs may be important in the inflammatory process of ATIN. The number of myeloid DCs in ATIN is significantly higher than that in lupus nephritis, whereas the number of plasmacytoid DCs is similar in these two diseases, suggesting DC subsets may be differentially involved in the pathogenesis of ATIN and lupus nephritis.

1619 Castleman's Disease and the Renal Biopsy: A Clinicopathologic Case Series

L Nicholas Cossey, Shree Sharma, Manisha Singh, Neriman Gokden. Nephropath, Little Rock, AR; University of Arkansas for Medical Sciences, Little Rock, AR.

Background: Castleman's disease (CD) is characterized by angiofollicular lymph node hyperplasia and increased serum IL-6 and VEGF. Renal involvement is uncommon and current knowledge is largely based on case reports. We present the first case series showing a spectrum of clinicopathologic and renal biopsy findings in CD.

Design: The databases from 2 centers were searched (2001-2014), retrospectively, and 7 patients with renal biopsies at the time of CD diagnosis were identified.

Results: See Table 1.

Case #-Age/ Sex/ Race	Clinical Presentation/ Serum Creatinine (mg/dl)	Serology	Renal Biopsy Diagnosis	Immuno-fluoresence	Electron Microscopy	Treatment
1- 39/ M/ W	ARF/ Increased	Neg	TMA	Neg	-Swollen ECSE lucency	S, R
2- 57/ M/ W	NRP/1.1	Neg	MPGN	Neg	-Swollen ECSE lucency	S,R
3- 56/ F/ W	NS, hematuria/ 3.0	High VEGF, IL-6	MPGN	Neg	-SE lucency-Mesangial interposition	R
4- 47/ M/ H	ARF, hematuria/ 12.7	High IgGLow C3, C4	IgG4-related TIN	TBM + for IgG, C1q, K, L	No EM	S
5- 37/ F/ W	NS/0.8	Hepatitis C	Minimal change disease	Neg	Diffuse foot processeffacement	S
6- 70/ F/ W	NS/1.2	Neg	Membranous Glomerulopathy	GBM + for IgG(3+), C3(2+), PLA2R(3+)	SE and IM deposits	Unk
7- 19/ M/ W	ARF/3.9	ANA (1:160)High VEGF, IL-6	TMA	Neg	-SE lucency Mesangiolysis	Unk

Abbreviations: Cau-Caucasian, His-Hispanic, ARF-acute renalfailure, NRP- nephrotic range proteinuria, NS-nephrotic syndrome, N-Normal, Neg-negative,TIN- tubulointerstitial nephritis, TMA-thrombotic microangiopathy, MPGN-membranoproliferativeglomerulonephritis, TBM-tubular basement membrane, GBM- glomerular basementmembrane, SE-subendothelial, IM-intramembranous, EC-endothelial cell, S-steroids,R-rituximab.

Conclusions: This case series shows a wide range of renal injury in patients with CD. MPGN and TMA have been described in CD in case reports and may be secondary to increased circulating VEGF and IL-6. The remaining cases in our series show diseases uncommonly seen in CD. These diseases may represent previously undescribed associations with CD or may be unrelated co-occurrence and further studies are required.

1620 Quantitative Shotgun Proteomics Analysis of Amyloid From Paraffom-Embedded Tissue

Dao-Fu Dai, Han-Yin Yang, Charles Alpers, Michael Maccoss, Kelly Smith. University of Washington, Seattle, WA.

Background: Subtyping of amyloidosis is often performed using immunohistochemistry, which can be problematic because of high background staining, epitope loss caused by formalin fixation and lack of optimal antibodies. Furthermore, inter-observer and inter-institution variability for these immunohistochemial tests may contribute to variability in diagnosis. A qualitative mass spectrometry test for subtyping amyloid has been developed at the Mayo clinic and other institutions. However, the qualitative test for amyloid subtyping is based solely on identification of peptide spectra and therefore has an element of subjectivity.

Design: We performed quantitative label-free shotgun proteomics analysis on paraffin-embedded tissue in cases with amyloidosis (n=36, including kidney and heart). Laser capture microdissection was performed to isolate tissue infiltrated by Congo red positive amyloid, followed by trypsin digestion, liquid chromatography and mass spectrometry (MS) using a Thermo Scientific Velos. High resolution MS data was obtained. MS/MS spectra were searched by SEQUEST. MSDapl was applied for quantitative measurement using normalized spectral abundance factor.

Results: Spectral abundance analysis revealed various mixtures of amyloidogenic proteins among the most abundant proteins in the Congo-red positive sections. In most cases of amyloidosis, in addition to the peptides corresponding to the subtypes of the amyloid, various additional amyloidogenic proteins were abundant, including serum amyloid P component (APSC), apolipoproteins A and E, and transthyretin. In cases of amyloid A and transthyretin amyloidosis, peptides corresponding to serum amyloid A and transthyretin were often the most abundant peptides. In cases with the clinical diagnosis of light chain amyloidosis, peptides corresponding to either lambda or kappa light chains were highly abundant but not necessarily the most abundant peptides.

Conclusions: Unbiased shotgun proteomics reveals mixtures of various amyloidogenic proteins in the Congo-red positive sections. Peptides corresponding to the subtypes of the amyloidosis are not necessarily the most abundant amyloidogenic peptides. Our data suggests that clinical correlation and comparison of peptide abundance with non-amyloid controls are required if the suspected subtype is not the most abundant amyloidogenic protein. Future experiments are being designed to develop sophisticated quantitative methods to identify the peptide patterns ("molecular signatures") for more objective and accurate subtyping of amyloid.

1621 The Role of Syndecans 1 and 4 in Podocyte-Glomerular Basement Membrane Interactions

Angela DiPoto-Brahmbhatt, Deborah Wassenhove-McCarthy, Kevin McCarthy. Louisiana State University Health Sciences Center, Shreveport, LA.

Background: Identifying key pathways that contribute to the development and progression of CKD/ESRD is vital for improving theraepeutic interventions that mitigate patient morbidity/mortality. The glomerular podocyte is known to be a critical determinant in glomerular homeostasis. Podocyte-matrix interactions have been shown to play an important role in this process. Recent studies from our laboratory demonstrated that heparan sulfate glycosaminoglycans (HS) play an important role in podocyte-matrix interactions. The results suggested that two members of the syndecan cell surface proteoglycan family (Sdc1 and Sdc4) mediate this interaction via engagement of their HS chains with the glomerular basement membrane. Our hypothesis for the current study is that the combinatorial signaling into the podocyte via both Sdc1 and Sdc4 is critical for glomerular homeostasis, but Sdc1 and Sdc4 may play different roles in the process.

Design: To explore our hypothesis, Sdc1 knockout (KO) and Sdc4 KO mouse models were used, and age matched C57BL6/J mice served as controls. Kidneys were harvested at 6mo and 1yr of age for light (PAS staining) microscopy, transmission electron microscopy (TEM), and immunofluorescence staining of frozen sections for podocyte markers (nephrin and synaptopodin). Kidneys were also labeled with polyethylenimine (negative charge indicator), and the number of particles/500nm were counted using TEM to evaluate potential differences in the contribution of each syndecan to the anionic charge of the glomerular basement membrane.

Results: Significant foot process effacement was absent in both Sdc KO mouse models. In Sdc4 KO glomeruli, nephrin staining accumulated within the podocyte cell body; this was not seen in the glomeruli of Sdc1 KO mice. Synaptopodin staining was comparable in both models. Sdc1 and Sdc4 KO mice developed prominent vacuoles in the proximal tubules at 6 mo, but at 1 yr of age the vacuoles disappeared. PAS stained kidney sections from Sdc4 KO mice at 6 mo showed the development of mild mesangial matrix expansion (ME) which progressed over time. The Sdc1 KO glomeruli did not develop ME. PEI labeling showed no change in anionic charge density in the Sdc4 KO animals, but a significant decrease in charge density was seen in the Sdc1 KO animals.

Conclusions: Our results show that differences exist between the Sdc1 and Sdc4 KO mouse models with regard to nephrin immunostaining, anionic charge density and mesangial expansion. Our results suggest that each proteoglycan species may play complementary but not redundant roles in glomerular homeostasis.

1622 Renal Allograft Granulomatous Interstitial Nephritis: An Uncommon Histologic Pattern With a Diverse Etiologic Spectrum

Alton Farris, Carla Ellis, Thomas Rogers, Shane Meehan. Emory University, Atlanta, GA; University of Chicago, Chicago, IL.

Background: Granulomatous interstitial nephritis (GIN) can present in renal biopsies; however, literature descriptions of this are somewhat limited. We sought to expand upon the literature to more completely understand the etiology of allograft GIN.

Design: Potential allograft GIN cases were retrieved from the pathology information systems of 2 academic medical centers. GIN cohort inclusion criteria required a mixed interstitial inflammatory infiltrate with at least 1 focal circumscribed aggregate of epithelioid macrophages and/or giant cells. Available clinical and pathologic data were compiled.

Results: GIN was present in 21 biopsies from 20 patients (14 males and 6 females) with a mean age of 48 years (standard deviation = 17, range = 22 to 77 years). The patients consisted of 9 African Americans, 6 Caucasians, 1 Hispanic, and 1 Asian; information was limited in 3 external consultative cases. At 1 center, among approximately 5,000 transplant biopsies, 10 had GIN, suggesting a prevalence of approximately 0.2%. GIN appeared at a mean of 513 days post transplant (median=132, standard error (SE)=321, range=10 – 5,898). Creatinine at biopsy averaged 3.5 mg/dL (SE=0.4, range=1.8 –

7.8). Infection, present in 10 cases, included adenovirus (n=2), polyomavirus (n=1), mycobacteria (n=2), *Candida albicans* (n=1), *Cryptococcus neoformans* (n=1), and bacterial urinary tract infection with features of megalocytic interstitial nephritis (n=3). Drug hypersensitivity was the likely etiology in 6 cases, including bactrim, dapsone, and foscarnet in 1 biopsy each and an unknown drug in 3 cases. One had recurrent granulomatosis with polyangiitis. In 4 cases, no firm etiology could be established. Seven of the biopsies also had features of rejection, including acute cellular rejection (ACR), type 2A (n=3); ACR, type 1B (n=2); ACR, type 1A (n=1); and concurrent ACR, type 1A, and antibody-mediated rejection (n=1). Ancillary studies utilized in selected cases included acid-fast bacillus, Grocott Methenamine Silver, and immunohistochemistry for adenovirus and the SV40 antigen. Follow-up, available in 15 patients, showed that 9 were alive with functioning grafts, 4 were alive with graft failure, 1 died with a functioning graft, and 1 died with graft failure.

Conclusions: Allograft GIN has a broad etiologic spectrum and is relatively uncommon at 0.2% of biopsies. Graft failure was frequent at 33%. Close clinicopathologic correlation and utilization of ancillary studies are needed for correct diagnosis and therapy.

1623 Spectrum of Glomerulopathy in Patients With Hepatitis C Infection

Mercia Jeanne Gondim, Dibson Gondim, Carrie Phillips. Indiana University, Indianapolis, IN.

Background: Over three million people in the United States (U.S.) are chronically infected with hepatitis C virus (HCV) of which a subpopulation develop kidney disease. HCV has been linked to a spectrum of glomerulopathies, most notably membranoproliferative glomerulonephritis (MPGN). We suspected a lower incidence of MPGN in our predominantly Midwest USA population of HCV+ patients due to comorbid factors including diabetes mellitus (DM). We report the histopathologic profile of HCV+ patients who had a renal biopsy specimen evaluated at our institution.

Design: Our university-based databank of surgical pathology reports was searched over a 22-year period for kidney biopsy specimens. We selected for study those patients with a history of HCV infection regardless of acute or chronic stage. Specimens were examined by brightfield, immunofluorescent (IF) and/or electron microscopy.

Results: From more than 7,000 renal biopsy specimens we identified 230 (3%) patients with a history of HCV infection, including 175(76%) males and 55(24%) females, with a mean age of 51 years (range 21 to 84 years). Mean serum creatinine at time of biopsy procedure was 4.05 mg/dL. Diagnoses included diabetic glomerulosclerosis 63 (27%), focal segmental glomerulosclerosis 48 (FSGS, 21%) of which 3 were HIV-positive, MPGN type 1 30 (13%), IgA nephropathy 20 (9%), membranous glomerulopathy 14 (6%), one was hepatitis B virus positive, and fibrillary glomerulopathy 3(1%). Only 4 patients had cryoglobulinemic glomerulonephritis.

Conclusions: Our renal biopsy specimens from HCV+ patients showed a wide distribution of glomerular disease, which justify the necessity of tissue examination. MPGN was not the most commonly encountered diagnosis. More than one-quarter had diabetic glomerulosclerosis, which correlates to the high prevalence of DM in the U.S., especially older patients like those in our study who are more likely to develop type II DM. One-fifth had FSGS of which the majority were HIV-negative. In conclusion, DM and other risk factors may play a more important role in the development of kidney disease in HCV patients rather than the virus itself.

1624 IgG Subclass Staining in Routine Renal Biopsy Material

Jessica Hemminger, Gyongyi Nadasdy, Anjali Satoskar, Sergey Brodsky, Tibor Nadasdy. Ohio State University Wexner Medical Center, Columbus, OH.

Background: Immunofluorescence staining plays a vital role in nephropathology, but the panel of antibodies used has not changed for decades. Further classification of IgG-containing immune-type deposits with IgG subclass staining (IgG1, IgG2, IgG3, IgG4) has been shown to be of diagnostic utility in various glomerular diseases, but their value in the evaluation of renal biopsies has not been addressed systematically in large renal biopsy material.

Design: Between January 2007 and June 2014, using direct immunofluorescence, we stained every renal biopsy for the IgG subclasses, if there was moderate to prominent glomerular IgG staining and/or IgG predominant or codominant glomerular staining by routine direct immunofluorescence.

Results: The total number of biopsies stained for IgG subclasses was 1,141, which included 391 membranous glomerulonephritis (MGN), 306 lupus nephritis, 77 fibrillary glomerulonephritis, 52 proliferative glomerulonephritis with monoclonal IgG deposits (PGNMIGD), 24 cryoglobulinemic glomerulonephritis, 22 anti-glomerular basement membrane disease, among others. We found that monoclonality of IgG deposits cannot be reliably determined based on kappa and lambda light chain staining alone, particularly if concomitant (frequently nonspecific) IgM staining is also present. PGNMIGD cannot be diagnosed without IgG subclass staining. In PGNMIGD, the glomerular morphology frequently has a membranoproliferative pattern and without IgG subclass stains the diagnosis of "idiopathic" membranoproliferative glomerulonephritis may be made. In IgG heavy and heavy and light chain deposition disease (10 cases), the subclass staining is very helpful. IgG subclass staining is useful in differentiating primary MGN (usually IgG4 dominant) from secondary MGN (usually IgG1 dominant). In proliferative glomerulonephritis with polyclonal IgG deposition, IgG1 dominance/codominance with concomitant IgG3 and IgG2 but weak or absent IgG4 staining favors an underlying autoimmune disease (such as SLE).

Conclusions: IgG subclass staining is a very useful diagnostic method in a selected cohort of renal biopsies, particularly in biopsies with glomerulonephritis with monoclonal IgG deposits and in monoclonal heavy and heavy and light chain deposition disease. Renal pathology laboratories should be capable of performing IgG subclass stains in renal biopsies with IgG deposits.

1625 Glomerular Injury Patterns as Recognized By Multiphoton Microscopy in Fixed Tissue Sections

Manu Jain, Steven Salvatore, Binlin Wu, Sushmita Mukherjee, Surya Seshan. Weill Cornell Medical College, New York, NY.

Background: Multiphoton microscopy (MPM) is a novel diagnostic modality which relies on intrinsic tissue emission to rapidly generate sub-cellular, histological resolution images from the tissues. Benefits of MPM include rapid, histologic assessment of tissue samples, without processing which preserves the tissue for further studies. MPM has not been studied in the setting of medical renal biopsies.

Design: Unstained deparaffinized sections of previously diagnosed cases of glomerular injury (n=38; 3 cases per lesion) were imaged with 25x objective and digital zooms (2, 3 and 5x). Signals were collected from autofluorescence (AF) and second harmonic generation (SHG) in separate channels and color coded.

Results: Normal glomerulus had AF mainly arising from non-fibrillary collagen IV, present in glomerular basement membrane (GBM) and the mesangium. Glomerular cells were visible having nucleus (low or no AF) with scant autofluorescent cytoplasm. Distinctive MPM findings included no glomerular abnormalities in minimal change and thin GBM disease, a non-proliferative pattern in membranous glomerulonephritis (MGN), FSGS, diabetic nephropathy (DN) and amyloidosis, and a proliferative pattern in membranoproliferative (including lobulation) and diffuse proliferative glomerulonephritis (GN). In MGN, thickening of capillary basement membrane (strong AF) was seen. In FSGS and crescentic GN, segmental sclerosis or cellular crescents were identified. In DN, mesangial nodules had a weaker AF as compared to more uniform, dense/strong AF in amyloid. MPM could not detect immune deposits. Interstitial collagen had SHG and was distinct from the collagen (I, III) present in normal glomerulus or sclerosis of FSGS (AF).

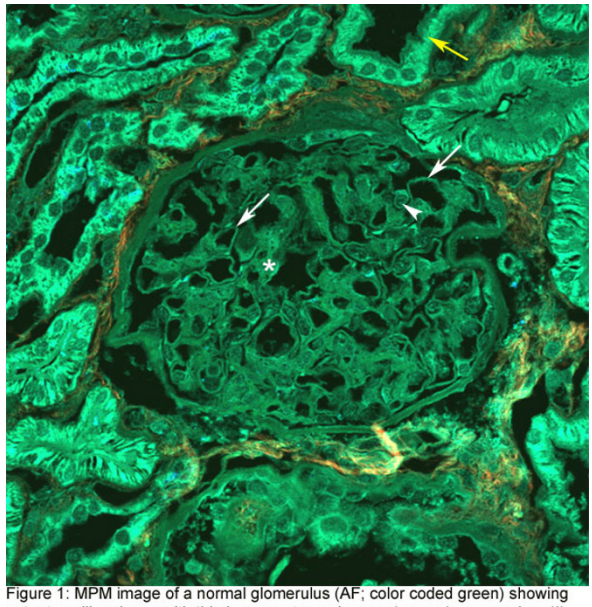

Figure 1: MPM image of a normal glomerulus (AF; color coded green) showing patent capillary loops with thin basement membranes (arrows), mesangium (*) and cells.Surrounding tubules (yellow arrow) and scant interstitium (SHG; color coded red) are also identified.Total magnification: 300x.

Conclusions: For the first time, we characterized the unique signatures and patterns of various glomerular pathology on MPM in fixed tissue sections. This knowledge can be translated to image fresh kidney biopsies (similar signatures as fixed tissue) for rapid identification of glomerular injury pattern particularly in urgent cases, to enable rapid therapeutic decisions without compromising the tissue sample which may be triaged appropriately for special diagnostic tests or molecular studies after MPM.

1626 Endothelial Activation and Lymphangiogenesis in Humoral Rejection of Kidney Transplants

Meghan Kapp, Sharon Phillips, Deborah Crowe, Jorge Garces, Agnes Fogo, Giovanna Giannico. Vanderbilt University, Nashville, TN; DCI Transplant Immunology Laboratory, Nashville, TN; Ochsner Health System, New Orleans, LA.

Background: Peritubular capillary (PTC) C4d is a specific but insensitive marker of antibody-mediated rejection (AMR). The 2013 Banff Conference revised AMR criteria to include C4d-negative AMR with evidence of endothelial-antibody interaction. Lymph vessel density is increased near cellular infiltrates in renal biopsies with acute T cell-mediated rejection.

We hypothesize that endothelial activation and lymphangiogenesis are increased with microcirculation injury (MI), positive serum donor-specific antibodies (DSA) and negative C4d, and correlate with intra-graft Tregs and Th17.

Design: Imunohistochemistry (IHC) for endothelial activation [P- and E- selectins (SEL)], lymphangiogenesis (D240), Tregs (FOXP3), and Th17 (STAT3) was performed on 73 renal specimens [28 AMR, compared to 19 with MI and DSA but negative C4d (-C4d), 11 with MI and DSA but minimal/focal C4d (m/fC4d), 15 with negative DSA and C4d with varying histologic diagnoses with positive MI in 73% of these (MI) and 7 normal nontransplant control cases (NL)].

Microvessel and inflammatory infiltrate density in interstitium and peritubular capillaries was assessed morphometrically with ScanScope CS, Aperio. Statistical analysis was performed using Kruskal-Wallis and Wilcoxon rank-sum tests.
Results: Microvessel density for P-SEL, E-SEL, and D240 was significantly elevated in AMR, -C4d, m/fC4d and MI compared to NL. P-SEL was significantly increased in AMR compared to MI. FOXP3 and STAT3 were significantly elevated in all groups vs NL.
Increased P-SEL, E-SEL, D240 expressions were significantly associated with increased FOXP3 and STAT3 expressions and graft failure.
Conclusions: Microvessel and lymphatic vessel density was significantly increased in DSA+ patients with MI, over a range of PTC C4d expression from negative to >50%, and in patients without C4d and DSA but with MI. Microvessel density was significantly associated with intragraft levels of FOXP3 and STAT3, and with graft failure. IHC evaluation of endothelial activation and lymphangiogenesis may supplement histologic findings of MI in minimal/focal C4d cases, and identify grafts at high risk of failure. Endothelial activation and lymphangiogenesis associated with AMR could aid in identification of potential therapeutic targets.

1627 Clinical Significance of CD44 Expression in Renal Biopsies of IgA Nephropathy Patients

Sewha Kim, Hyeon Joo Jeong. Yonsei University College of Medicine, Seoul, Republic of Korea.
Background: CD44 is a glycoprotein expressed in activated parietal epithelial cells (PECs) lining Bowman's capsule. It has been shown that migration of CD44+ PECs to the glomerular capillaries is an early step in the process of developing sclerotic lesion in segmental glomerulosclerosis (SS).
Design: To assess the clinical implications of CD44 expression in mild IgA nephropathy (IgAN), CD44+ PECs and visceral epithelial cells (VECs) were quantificated on the immunostained slides of 126 renal biopsies. They were grouped as follow: group A (Hass class I, n=30), B (Haas class III without SS or adhesion, n=31) and C (Haas class III with SS or adhesion, n=65).
Results: Both CD44+ PECs (p=0.049) and VEC (p=0.014) were most frequently observed in group C .

CD44 positive	Group A	Group B	Group C	p-value
PEC+ (%)	21 (70.0)	22 (71.0)	57 (87.7)	0.046
VEC+ (%)	12 (40.0)	17 (54.8)	46 (70.8)	0.014
PEC+ or VEC+ (%)	21 (70.0)	23 (74.2)	59 (90.8)	0.018
PEC and VEC/G	0.89	0.89	2.23	0.109

At the time of biposy, as the number of CD44+ VECs increased, serum Cr (p=0.046) and UP/Cr (p=0.010) increased and eGFR (p=0.014) decreased in the groups without segmental lesions (A and B). When three groups were combined, UPCr at the last follow-up significantly increased, as the sum of CD44+ PECs and VECs increased (p=0.006).

Group A and B	CD44+ VEC/G	CD44+ VEC >=1	p-value
sCr (mmol/L) biopsy	0.82	1.01	0.046
sCr (mmol/L) last FU	0.85	1.01	0.096
eGFR (mL/min) biopsy	94.6	71.8	0.010
eGFR (mL/min) last FU	94.9	72.0	0.067
UP/Cr biopsy	0.91	3.6	0.014
UP/Cr last FU	0.36	0.41	0.813
Group A, B and C	CD44+ PEC and VEC/G	CD44+ PEC and VEC/G >=1	p-value
sCr (mmol/L) biopsy	0.90	0.91	0.808
sCR (mmol/L) last FU	0.89	1.03	0.147
eGFR (mL/min) biopsy	88.1	93.4	0.232
eGFR (mL/min) last FU	88.3	80.7	0.139
UP/Cr biopsy	0.90	1.52	0.062
UP/Cr last FU	0.42	0.84	0.006

Conclusions: In conclusion, CD44 expression in VEC or PEC was associated with IgAN with segmental lesion and worse profiles of renal function. It reflects that CD44 expression is involved in the deterioration of renal function in IgAN.

1628 Podocyte Infolding Glomerulopathy – Occurrence of the Disease Entity in the United States, and the Potential Role of an Autoantibody

Pavel Kopach, Cathryn Byrne-Dugan, Laurence Beck, Vanesa Bijol, Monika Pilichowska, Helmut Rennke, Masha Bilic. Boston University Medical Center, Boston, MA; Tufts Medical Center, Boston, MA; Brigham & Women's Hospital, Boston, MA.
Background: Podocyte infolding glomerulopathy (PIG) is a rare disease entity previously described as "nuclear pore complex" deposition [1]. On silver stain it mimics membranous nephropathy with fine vacuolization or "bubbling" of the glomerular basement membrane. The process is sometimes but not always associated with immune complex deposits. In the largest study to date of 25 cases of PIG in Japan, most patients presented with sub-nephrotic proteinuria and preserved renal function [1]. The majority of the patients had either a concomitant diagnosis of SLE or other autoimmune disease [1]. Patients treated with immunosuppression showed a decrease in proteinuria. We hypothesize that PIG is caused by a circulating autoantibody that targets podocytes or glomerular proteins.
Design: We describe 6 cases of PIG from 3 institutions in Boston over the past 5 years and investigate the role of an autoantibody in the pathogenesis of PIG.
Results: Five out of six cases were females with an age range of 27-71 year old and one was a 70 year old male. Two cases had a concomitant diagnosis of SLE, and one had undifferentiated connective tissue disorder. Five cases had a positive ANA. Proteinuria ranged from 1.7 to 12.2 g/day, and was nephrotic-range in 4 patients. Serum creatinine ranged from 0.4 to 2.66 mg/dl. Complement levels were low in two cases. The predominant pattern of injury by light microscopy was membranous, except for the case with concomitant anti-GBM disease which presented with crescentic glomerulonephritis. Immunofluorescence microscopy showed no to minimal reactivity for immunoglobulins, complement, and fibrin components in all cases except for the case of anti-GBM. Ultrastructurally all cases showed both podocyte infolding and microsphere formation. Serum from case #1 was analyzed against extractable human glomerular proteins via Western blot. We found intense reactivity, with both IgG1 and IgG4, for a band in the 55-60 kDa size range. This did not appear to correspond with any previously known antigen.
Conclusions: PIG is a rare disease entity, which mimics membranous nephropathy and can be easily missed. An autoantibody is likely involved.
Reference:1.Joh K, Taguchi T et al. Proposal of podocyte infolding glomerulopathy as a new disease entity: a review of 25 cases from nationwide research in Japan. Clin Exp Nephrol. 2008 Dec; 12(6): 421-31.

1629 Infection Related Glomerulonephritis ia an Important Cause for Acute Kidney Injury / Rapidly Progressive Renal Failure in Diabetic Patients in India

Anila Kurien. Center for Renal and Urological Pathology, Chennai, Tamil Nadu, India.
Background: Patients with diabetes have increased risk for acute kidney injury (AKI) when compared with patients without diabetes. AKI and rapidly progressive renal failure (RPRF) in a diabetic patient may have various aetiologies. This study evaluates the renal biopsy findings in diabetic patients presenting with acute kidney injury or rapidly progressive renal failure.
Design: Among the 3059 native kidney biopsies received in the past one year, 516 biopsies (16.9%) were from diabetic patients. Of these, 110 patients (21.3%) presented with acute kidney injury or rapidly progressive renal failure. Histopathologic features of these 110 patients were analysed. Biopsy findings were classified into 3 groups: Group I, isolated non diabetic renal disease (NDRD); Group II, NDRD with underlying DN; and Group III, with only DN.
Results: Among the 110 patients (M:F=3.4:1, mean age 56.4yr) who presented with AKI/RPRF, 45 (40.9%) were in Group I, 40 (36.4%) in Group II and 25 (22.7%) in Group III. Acute tubular injury (ATI) was the most common diagnosis (37.8%) in Group I followed by infection related glomerulonephritis (IRGN)(15.6%) and acute interstitial nephritis (13.3%). Three out of the 7 patients who had isolated IRGN had undergone crescentic transformation at the time of biopsy. The other findings included IgA nephropathy (9%), ANCA associated crescentic glomerulonephritis and collapsing glomerulopathy (4.4% each), cast nephropathy, acute pyelonephritis, amyloid AL, anti-GBM disease, cortical necrosis, cryoglobulinemic glomerulonephritis and sarcoidosis (2.2% each). ATI superimposed on DN accounted for half the diagnosis in Group II, followed by IRGN on DN (30%). Among the patients without a NDRD the most common histological class was Class 3 (48%) followed by Class 4 DN (36%) and Class IIa and Class IIb(8% each).
Conclusions: NDRD alone or superimposed on DN was seen in more than 75% of biopsies performed for AKI/RPRF. Acute tubular injury was the most common biopsy finding. Infection related glomerulonephritis is emerging as an important cause for AKI/RPRF in diabetic patients in India, an observation that has not been reported previously from other countries.

1630 Immunohistochemical Analysis of Myoglobin Cast Nephropathy in Renal Biopsies

Helen Liapis, Randolph Hennigar, Joseph Gaut, Fred Silva. Nephropathology Associates, Little Rock, AR.
Background: Myoglobin (myo) release into the circulation (i.e., rhabdomyolysis) may promote serious and life threatening acute kidney injury. The morphology of myo-related kidney injury is nonspecific and typically manifests as acute tubular injury with globular, granular and/or cellular casts, oftentimes with atypical features. Immunohistochemistry (IHC) using antisera against myo enhances detection and imparts greater specificity to the diagnosis. Accordingly, we analyzed a large series of renal biopsies from patients suspected of myo-related injury by correlating clinical parameters, basic morphology and IHC staining patterns.
Design: A total of 27,850 consecutive renal biopsies accessioned between January 2011 and June 2014 were screened for myo using IHC. IHC was performed using rabbit anti-human myo antisera (Cell Marque, Rocklin, California 95677) in a conventional automated procedure. Only intensely stained casts were considered positive.
Results: Of 27,850 renal biopsies, 580 (2%) were immunostained for myo based upon for clinical and/or morphologic suspicion for myo-related kidney injury. A total of 238 (41%) cases were found to be positive for myo casts by at least one experienced renal pathologist. The average age of patients was 48.6 yrs (range 15-87); 154 males and 84 females. All patients presented with acute renal failure (average SCr 9.6 mg/dL; range 2.2-45.0) and various comorbidities including polydrug substance abuse, adverse medicinal reactions, dehydration, infection, sepsis, intense exercise, trauma, and other underlying kidney diseases. The morphology of the myo casts ranged from

dirty slightly brown granular casts by H&E, to beaded globular casts that stained brightly fuchsinophilic with Masson trichrome and partially argyrophilic with silver methenamine. Approximately 10% of myo positive biopsies showed calcium oxalate or phosphate. All cases displayed acute tubular injury associated with intratubular debris and thinning and vacuolization of tubular epithelium. Positive myo staining was observed occasionally in distal tubular epithelium. One case showed concurrent myeloma cast nephropathy and myoglobin casts.
Conclusions: We present the largest renal biopsy series of myo-associated renal disease. Myo IHC in renal biopsies with tubular casts associated with acute tubular injury effectively distinguishes rhabdomyolysis from other types of protein casts. The cast morphology tends to be granular or beaded-globular and stains fuchsinophilic on trichrome and argyrophilic on silver methenamine.

1631 Podocyte Invagination into Glomerular Basement Membranes Is Associated With Proteinuria, Diabetes Duration, and Tubulointerstitial Fibrosis in Diabetic Nephropathy

Mercury Lin, Behzad Najafian. University of Washington Medical Center, Seattle, WA.
Background: Diabetic nephropathy (DN) is by far the leading cause of end stage renal disease. Proteinuria is a known adverse prognosticator of DN. We aim to examine if glomerular basement membrane (GBM) ultrastructural abnormalities are associated with proteinuria in diabetic patients.
Design: 34 consecutive clinical biopsies with DN from our institution with available electron micrographs were retrospectively reviewed. Biopsies with concomitant other glomerulopathies were excluded. The observer was masked to clinical data. Ultrastructurally, the glomerular capillary walls are examined for the following features: (1) invagination of podocyte foot process into GBM, defined as of greater than 1/2 of thickness of affected GBM, and (2) complete GBM break that is covered by podocytes. Mesangial expansion, arteriosclerosis, arteriolar hyalinosis, and interstitial fibrosis and tubular atrophy (IFTA) were semiquantitatively scored (0-3). Clinical data were extracted from medical charts.
Results: 49 [16-108], median [range], glomerular capillary loops from 2 [1-4] glomeruli are examined per biopsy. 26/34 biopsies (76%) showed podocyte invagination into GBM (0.04 invaginations/capillary loop [0.01-0.14]). 13/34 biopsies (38%) showed podocyte covering complete breaks in the GBM (0.03 breaks/capillary loop [0.1-0.5]). Subjects with >0.05 invaginations/capillary loop (~ 30th top percentile) had longer diabetes duration (p=0.002), greater urine protein creatinine ratio (p=0.029), and IFTA (p=0.045). Virtually all biopsies with GBM breaks covered by podocytes also had podocyte invagination. Podocyte invaginations and GBM breaks were also more commonly seen in type 1 vs. type 2 diabetics (p=0.008and 0.002, respectively). However, diabetes duration was also greater in type 1 diabetic patients in this study (p=0.03) Interestingly, in 3/34 cases we observed thin GBMs bridged over the complete breaks.
Conclusions: Our study suggests that glomerular basement membrane ultrastructural abnormalities progressively increase with diabetes duration and are related to proteinuria and chronic injury. Invagination of podocytes into glomerular basement membranes may contribute into proteinuria with creating shunts bypassing one essential layer of the glomerular filtration barrier. GBM breaks covered by podocytes may evolve into formation of capillaries with thin GBM, occasionally observed in DN. Further studies are ongoing to explore significance of this phenomenon.

1632 Renewed Pathological Findings in Cadmium Nephropathy of Itai-Itai Disease – Characteristic Impairment of the Superficial Nephrons and Proximal Tubules

Fukuda Mai, Yurie Kazumi, Hiroki Yonezawa, Mizuki Ueno, Chikage Minagawa, Syo Ikeda, Koichi Tuneyama, Johji Imura, Yoshihiko Ueda. Graduate School of Medicine and Pharmaceutical Sciencies, Toyama, Toyama, Japan; Koshigaya Hospital of Dokkyo Medical School, Koshigaya, Saitama, Japan.
Background: Disorders of various organs may be caused by the prolonged oral ingestion of heavy metals, such as cadmium (Cd). The main target organ of Cd toxicity is the kidneys, and epithelial damage of the proximal tubules is particularly characteristic. The abnormalities of calcium metabolism caused by tubular extinction and subsequent osteomalacia are essential important mechanisms in "itai-itai disease" (IID). Here, we report that lesions in the outer layer nephrons and changes in peritubular capillary networks associated with superficial nephrons were specifically found in IID.
Design: Paraffin embedded sections of renal tissues were obtained from a total of 98 autopsied cases of IID. The sections were stained with hematoxylin-eosin and the degree of stromal fibrosis was examined by Masson trichrome staining. Immunohistochemical analysis of capillaries by anti-CD34 antibodies and lymphatics by D2-40 antibodies was used to determine proliferation and regression status. In addition, a morphometrical study was used to perform semiquantification.
Results: Although the kidneys were markedly atrophic with a mean weight of 40 g, these mainly atrophic lesions were in the outer layer of the renal cortex. The hyalinization of nephrons was observed specifically along the outer layer. Interstitial fibrosis was also observed around the atrophic proximal tubule. Peritubular capillaries were markedly decreased in number and dilated lymphatic vessels became manifest.
Conclusions: Although there have been few previous reports on the disorder of nephrons in Cd nephropathy, this study demonstrated disorders of superficial nephrons were more specific for IID than for other renal diseases. Furthermore, the abnormalities of peritubular capillaries and lymphatic vessels in conjunction with the superficial nephron may become the key to elucidate the mechanism of this disease.

1633 Acute Vascular Lesions in the Kidney Transplant and Relationship To Cellular and Antibody-Mediated Rejection (ABMR)

Elizabeth Martinez, Agnes Fogo. Vanderbilt University Medical Center, Nashville, TN.
Background: Acute vascular rejection (AVR) may occur as a component of T-cell mediated rejection (TCMR) or in relation to ABMR. A recent study from Europe (Lancet 2013;381:313-19) indicated that isolated AVR (Banff) lesions were highly associated with ABMR. However, the threshold for Banff type I TCMR is much higher than that for CCTT type I TCMR. We investigated the occurrence of AVR in relation to concurrent TCMR by CCTT criteria, and the frequency of ABMR.
Design: All kidney transplant biopsies reviewed in our division between January 1, 2004 and September 30, 2014 were included. We identified transplant biopsies with the diagnosis of AVR, including CCTT Types II and III. We assessed the concurrence of acute cellular rejection by CCTT criteria (i.e. >5% interstitial inflammation, >3 tubules with tubulitis) and C4d immunostaining.
Results: Of the 3179 kidney transplant biopsies, 385 (12%) had AVR, CCTT Type II and/or III. Of these AVR cases, 167 (43%) had "isolated AVR" by CCTT criteria, with no concomitant CCTT Type I TCMR, and the remainder 218 (57%) had AVR+TCMR. C4d positivity in peritubular capillaries, a marker of ABMR, was present in 28% (42/152 tested) of our "isolated AVR" cases, contrasting 42% C4d positive "vascular rejection ("v" lesions)" as classified by Banff in the European Study. In patients with combined TCMR and AVR by CCTT criteria, C4d peritubular capillary staining was present in 30% (62/209).
Conclusions: We conclude that "isolated AVR" lesions are not exceedingly rare, occurring in 5% of all our transplant biopsies. Further, v lesions are "isolated" without concomitant TCMR by CCTT criteria in 43%. Evidence of ABMR by diagnostic C4d positivity is present in 28% of "isolated AVR", much less than when classified by Banff criteria. These findings suggest that current Banff ACR criteria might have a threshold too high to identify T-cell mediated immune injury in the transplant.

1634 Anti-Glomerular Basement Membrane Syndrome With Superimposed Immune Complex-Mediated Glomerulonephritis: Case Series of an Unusual Dual Pattern of Renal Disease By Light, Immunofluorescence, and Electron Microscopy Analysis

Gonzalo Mendez, Daisy Cisternas, Lizzet Fernandez, Lorena Henriquez. Pontificia Universidad Catolica de Chile, Santiago, RM, Chile.
Background: Anti-glomerular basement membrane glomerulonephritis (anti-GBM GN) has a well-defined morphological pattern of renal injury characterized by a necrotizing and crescentic glomerulonephritis. The immunofluorescence and ultrastructural features are quite unique, with linear deposition of IgG along the glomerular capillary walls, and no evident electron dense deposits at the glomerular tuft. The simultaneous association of anti-GBM GN with immune complex-mediated glomerulonephritis (IC-GN) is a rarely described and defined pathological condition.
Design: A retrospective analysis of renal biopsies diagnosed at our institution from 2000 to 2014 was performed. The pattern of glomerular injury, immunoglobulin deposition, and ultrastructural features were evaluated. The information on pertinent laboratory and clinical data was obtained.
Results: Among a total of 4680 native kidney biopsies, 16 cases of anti-GBM GN were identified (0.3%). Of these, 4 cases (25%) had a concurrent IC-GN. The light microscopy features were a focal necrotizing and crescentic glomerulonephritis in 2 cases, one of them showing endocapillary proliferation. The remaining 2 cases revealed a chronic crescentic glomerulonephritis. The immunofluorescence microscopy showed, in concurrence to linear IgG deposition, granular deposits at mesangium and capillary walls, of IgG and C3 (2), IgA and C3 (1) and IgA only (1). The ultrastructural analysis of both cases with IgG-C3 granular deposits revealed mesangial, subepithelial and intramembranous electron dense deposits. The case with IgA-C3 reactivity had small deposits at mesangium, and few at subendothelial and subepithelial spaces. The case with IgA reactivity showed electron dense deposits restricted to the mesangium. Significant clinical data was a sepsis from a foot cellulitis in the case with IgA-C3 deposits. Viral and other serological tests were negative for all cases.
Conclusions: The concurrence of anti-GBM GN and IC GN is a common finding. This dual pattern of immunoglobulin deposition probably relates to an exagerated antigen exposition due to extreme disruption of basement membranes in anti-GBM GN, and acting as new targets that favor a potential second-hit event of antibody deposition. A proliferative glomerulonephritis with subendothelial deposits, potentially infectious-related, might favor the overexposition of collagen epitopes, triggering the anti-GBM GN. We consider as coincidental the association with IgA nephropathy.

1635 Vascular Changes in Extrarenal Tissue Correlate With the Severity of Arteritis in Acute Cellular Rejection II and III

Alexei Mikhailov, Huaibin Mabel Ko, Fadi Salem. Mount Sinai Medical Center, New York, NY.
Background: The gold standard for the diagnosis of rejection in transplanted kidney is renal biopsy, a traumatic procedure with potential complications. We hypothesized that kidney vascular changes observed in acute cellular rejection will also be seen in the surrounding perirenal fat and renal capsule and will have a diagnostic significance.
Design: We studied the kidney biopsies performed at the Mount Sinai Medical Center from 2008 to 2014 diagnostic of borderline, acute (ACR) or chronic (CCR) cellular rejection and antibody mediated rejection (AMR) and selected those with arteriole-containing perirenal tissue present. The transplant rejection diagnosis was formulated and the pathological changes were quantified according to the Banff 97 Classification of Renal Allograft Pathology. For evaluation of extracapsular tissue, Hematoxylin and Eosin and Masson Trichrome stained slides were used. C4D staining intensity was graded from 0 to 3 according to the Banff 07 Classification of Renal Allograft Pathology. The significance of difference between patient biopsy groups was determined using single factor ANOVA.

Results: The perirenal tissue in petients with ACR types II and III showed the same spectrum of vascular changes as the corresponding kidney. The average perirenal intimal arteriolitis score in ACR IIA was 0.58 ± 0.27 (N=15), in ACRIIB- 1.33 ± 0.21 (N=12) and in ACRIII- 1.85 ± 0.5 (N=5). The difference between the groups was statistically significant (P<0.06). Perivascular lymphocytic infiltration in perirenal tissues was observed only in ACRIIB. The renal tissue of 13 patients with ACR I-III showed positive C4D staining grade I to 3. The intensity of this staining was inversely proportional to the ACR grade and did not correlate with the extrarenal vascular changes. CCR biopsies displayed lymphocytic infiltrates in the perirenal tissue but not vascular lesions (N=7). No perirenal arteriolitis was observed in acute borderline rejection, ACR IA ot IB (N=10 in each group). In 50% of cases with AMR (N=14) perirenal interstitial lymphocytic infiltrates were detected in the absence of arteriolitis.
Conclusions: Perirenal vasculitis is present specifically in acute cellular kidney transplant rejection of the vascular type (IIA-B and III). Thus, biopsies of the perirenal tissue which can be sampled more extensively to increase precision of diagnosis can be used to reduce the frequency of kidney biopsies in patients with known type II and III rejection.

1636 An Increased Level of Serum 1,25(OH)2-Vitamin D3 Alleviates Renal Tubulointerstitial Fibrosis Induced By Unilateral Ureteral Obstruction in Homozygous Klotho Mutant Mice

Yasuteru Muragaki. Wakayama Medical University, Wakayama, Japan.
Background: Previous studies have suggested that Klotho provides reno-protection against unilateral ureteral obstruction (UUO)-induced renal tubulointerstitial fibrosis (RTF). Because the existing studies are mainly performed using heterozygous Klotho mutant (HT) mice, we focused on the effect of UUO on homozygous Klotho mutant (*kl/kl*) mice.
Design: We performed UUO using WT, HT, and kl/kl mice and examined the degree of RTF. TGF-b1-induced epithelial mesenchymal transition (EMT) was evaluated in primary proximal tubular epithelial culture cells (PTECs) isolated from WT, HT, and kl/kl kidneys. The renal epithelial cell line NRK52E was used to examine the effect of TGF-b1-induced EMT when treated with a large amount of inorganic phosphate (Pi), FGF23, or calcitriol. kl/kl mice were fed vitamin D-deficient diet to examine the effect of Pi/Ca metabolism on RTF.
Results: UUO kidneys from HT mice showed a significantly higher level of RTF and TGF-β/Smad3 signaling than wild-type (WT) mice, whereas both were greatly suppressed in *kl/kl* mice. PTECs isolated from *kl/kl* mice showed no suppression in TGF-b1-induced EMT compared to those from HT mice. In NRK52E cells, a large amount of inorganic phosphate (Pi), FGF23, or calcitriol was added to the medium to mimic the *in vivo* homeostasis of kl/kl mice. Neither Pi nor FGF23 antagonized TGF-b1-induced EMT. In contrast, calcitriol ameliorated TGF-b1-induced EMT in a dose dependent manner. A vitamin D_3-deficient diet normalized the serum 1,25 $(OH)_2$ vitamin D_3 level in *kl/kl* mice and enhanced UUO-induced RTF and TGF-β/Smad3 signaling.
Conclusions: The alleviation of UUO-induced RTF in *kl/kl* mice was due to the TGF-b1 signaling suppression caused by an elevated serum 1, 25$(OH)_2$ vitamin D_3.

1637 Visualization of Podocyte Substructure With Structured Illumination Microscopy (SIM): A New Approach To Nephrotic Disease

James Pullman, Elaine Campbell, Jonathan Nylk, Frank Gunn-Moore, Michael Prystowsky, Kishan Dholakia. Montefiore Medical Center, Bronx, NY; University of St. Andrews, St. Andrews, Fife, United Kingdom.
Background: Currently only electron microscopy (EM) can resolve renal podocyte substructure. Structured Illumination Microscopy (SIM), a new optical technology, can resolve below the wavelength of visible light and also image in three dimensions (3D). With immunofluorescence (IF) staining, SIM has the potential to show podocyte substructure more rapidly than EM, and to localize specific proteins in the glomerulus in 3D. SIM may thus allow better and more rapid diagnosis of podocyte disease and give new insight into its cellular basis.
Design: We used SIM (Nikon n-SIM) to examine frozen sections of renal biopsies stained with IF markers for actin (phalloidin) and/or podocin (anti-podocin). All reagents were obtained from Sigma. We analyzed the podocyte cytoskeleton and its foot process structure in 2D and 3D images and compared them with electron microscopy (EM) in 3 normal biopsies and 6 with nephrotic disease, including minimal change disease (3), membranous nephropathy (2) and diabetic nephropathy (1).
Results: SIM of normal glomeruli in sections stained for podocin showed curvilinear patterns densely covering capillary walls, of similar dimensions and appearance to podocyte foot processes seen by EM. 3D display aided in seeing these patterns. Podocin staining of all nephrotic disease biopsies showed more sparse but often more intensely fluorescent segmental curved lines, corresponding to effaced foot processes seen by EM. There was also abundant punctate capillary wall staining for podocin not seen in normal glomeruli. Actin staining of normal glomeruli showed a capillary wall pattern similar to that for podocin, but which did not co-localize with it on double immunostaining. Additional actin staining was seen as branching short rods perpendicular to the capillary wall, correlating with major podocyte processes. Unlike podocin, there was little difference between actin staining in normal versus nephrotic disease glomeruli.
Conclusions: SIM can resolve podocyte substructure, including major cell processes and foot processes, as well as and more rapidly than EM. Podocin staining can distinguish normal glomeruli from those with nephrotic disease. The short, intensely stained podocin segments in nephrotic diseases could have defective filtration properties which could explain why proteinuria occurs even as filtration slits decrease in abundance. SIM of actin staining shows little or no difference between normal and nephrotic disease, suggesting other causes for foot process effacement.

1638 Next Generation Sequencing (NGS) of the T-Cell Receptor (TCR) for Differentiating T-Cell Mediated Rejection (TCMR) From BK Virus (BKV) Induced Inflammation in the Kidney

Parmjeet Randhawa, Y Huang, A Lesniak, G Zeng. University of Pittsburgh, Pittsburgh, PA.
Background: There is an unmet need to develop a test that can determine whether T-cell responses in BKV nephropathy (BKVN) are directed against viral antigens or alloantigens. The ability of a T-cell to respond in an antigen-specific manner is encoded in the sequence of the TCR hypervariable complementarity-determining region 3 (CDR3). Therefore, NGS of TCR aβ genes would be a logical solution to this problem.
Design: Biopsy genomic DNA was extracted from 6 patients with TCMR and 6 with a history of BKVN . A TCRβ CDR3 template library was generated using 45 TCR Vβ forward primers and 13 TCR Jβ reverse primers and submitted for NGS. Raw sequence data was preprocessed to remove technical errors and identify those sequences that had at least a 6-nt match to one of the 45 Vβ gene segments and one of the 13 Jβ gene segments. V- region, D-region and J-regions were identified by the ImMunoGeneTics IMGT/Junction Analysis tool . Rearranged CD3 sequences containing substitutions, insertions or deletions that result in frameshifts or premature stop codons were be regarded as nonproductive and excluded from analysis. In each sample the total number of unique TCR b CDR3 sequences (unique T-cell clones or clonotypes) was ranked by relative frequencies.
Results: Analysis of ten 25 micron sections per biopsy yielded a median of 36,179 TCR sequences (IQR 14,195 -153,641). Sequences starting from the Jβ segment tag consistently captured the complete CDR3 region, which has an average nucleotide length 35 +/- 3bp. Dendrograms revealed that V-gene, J-gene, and D-gene usage patterns were a function of HLA type. The 5 most abundant HLA-A2 reactive T-cell clones in TCMR had clonal frequencies varying from 0.0034-0.0436%. The corresponding CDR3 sequences did not overlap with the 5 most BKV large T antigen reactive T-cell clones, which had clonal frequencies ranging from 0.0025% to 0.0824% in BKVN. TCR-BV06 usage was associated with HLA-A2 reactivity while TCRBV18 and TCRBV27 were associated with T-cell response to BKV infection.
Conclusions: CDR3 sequences in T-cell clones sensitized to HLA-antigens are distinct from those seen in BKV sensitized T-cells. Determination of the respective clonotype frequencies could be potentially used to assign separate tissue scores for rejection and BKV associated inflammation. These scores could then guide more rational therapy of patients with biopsies that show pathologic changes difficult to interpret by standard light microscopy.

1639 The NEPTUNE Digital Pathology Protocol Increases Accurate Glomerular Number Assessment

Avi Rosenberg, Matthew Palmer, Lino Merlino, Jonathan Troost, Adil Gasim, Serena M Bagnasco, Carmen Avila-Casado, Duncan Johnstone, Jeffrey Hodgin, Catherine Conway, Jeffrey Kopp, Cynthia Nast, Laura Barisoni, Stephen Hewitt. Johns Hopkins University, Baltimore, MD; University of Pennsylvania, Philadelphia, PA; University of Miami, Miami, FL; University of Michigan, Ann Arbor, MI; University of North Carolina, Chapel Hill, NC; University Health Network, Toronto, ON, Canada; Temple University, Philadelphia, PA; Leica, Vista, CA; National Institute of Diabetes and Digestive and Kidney Diseases, Bethesda, MD; Cedars-Sinai Medical Center, West Hollywood, CA; National Cancer Institute, Bethesda, MD.
Background: Standardized reporting of renal biopsies is central to diagnosis and prognosis of medical kidney diseases. However, reproducibility is a challenge for basic metrics (i.e., glomerular number (GN) and % global sclerosis (GS)). The NEPTUNE digital pathology protocol (NDPP) seeks to standardize reporting metrics by refining scoring reproducibility. GN and GS reported by conventional light microscopy (LM) vs those obtained by digital annotation were compared through analysis of histologic levels on scanned whole slide images (WSI).
Design: 9,379 glomeruli in 274 cases with WSI (79 MCD, 111 FSGS, 51 MN, 33 IgA NP) from 21 centers were digitally annotated. Total or average GN/case and total number with GS were enumerated on WSI; reported GN (total or average) and glomerular number with GS were excerpted from the pathology reports.
Results: The discrepancy between reported vs annotated GN increased proportionally to the total GN. There was significant disease-dependent %GS difference between annotated and reported for IgA and FSGS. There was a significant mean discrepancy up to 14.6% in %GS in 30-80% GS bracket. Differences were observed across all centers.

Summary of glomerular enumeration (mean, **p

Reported as	Sample	Reported GN	Annotated GN	Reported GS (%)	Annotated GS (%)
Average	Overall	21	36**	15	17
	FSGS	19	35**	24	28**
	MCD	25	42**	1.2	1.3
	MN	18	25**	6.2	6.1
	IGA	13	24	37	42
Total	Overall	18	30**	14	16
	FSGS	18	30**	16	15
	MCD	21	38**	3	2
	MN	17	26**	9	9
	IGA	16	27**	29	40**

Conclusions: In contrast to LM, glomerular annotation on sequential WSI provides a more accurate and reproducible pathologic assessment. Compatible with this increased accuracy in glomerular counting we propose that WSI accrual and annotation of study-related biopsies will allow for improved quantitation of glomerular injury.

1640 Clinicopathologic Correlation of HIV-Associated Nephropathy (HIVAN): A Twenty-Year Retrospective Review and Comparison

Diane Saint-Victor, Vanesa Bijol, Jose Navarette, Thomas Rogers, Alton Farris, Arlene Chapman, Carla Ellis. Emory University Hospital and School of Medicine, Atlanta, GA; Emory University School of Public Health, Atlanta, GA.

Background: Further study is required regarding the clinicopathologic correlation and incidence of HIV-Associated Nephropathy (HIVAN). No prior study has looked specifically at how pathologic features associated with HIVAN, as well as its incidence, may have changed over time since the original descriptions of the disease and evolution of treatment strategies.

Design: A search of our pathology data system was performed. All patients diagnosed with HIVAN were reviewed in the 4 year period between 2010 and 2014, and analyzed in terms of demographic and clinical information (age, sex, and race) and pathologic features (degree of glomerular global collapse, segmental collapse, global sclerosis and segmental sclerosis). This analysis was compared to a prior, similar study between 1995 and 2004. In both groups, the pathologic findings were expressed as a percentage of the total number of glomeruli in each biopsy. Interstitial fibrosis and tubular atrophy (IFTA) and arteriosclerosis were graded as none, mild (<30%), moderate (30-60%) and severe (>60%). Incidence was calculated using the population of all Emory University patients receiving a kidney biopsy during the same period.

Results: A total of 25 confirmed cases were reviewed. The average age at time of diagnosis was 38 years (SD=12.9, median=38). Seventy-two percent of cases were male. All patients were African-American. The incidence of HIV-associated nephropathy (HIVAN) in Emory University patients between the years of 2010 and 2014 was approximately 578 per 100,000 (1,826 per 100,000 in earlier cohort). Among the recent cohort, neither global nor segmental sclerosis were correlated with eGFR at diagnosis. Presence of collapsed glomeruli was strongly correlated with eGFR less than 30 ml/minute/1.73 m^2 (0.004). Increased global sclerosis was correlated with higher proteinuria at diagnosis (p=0.037).

Conclusions: In our 4-year cohort with representative cases from a single institution, it appears that presence of collapsed glomeruli is associated with decreased eGFR, and that increased global sclerosis may be associated with higher proteinuria levels. Incidence of HIVAN, as compared to incidence from prior years at the same institution, has significantly decreased, which may be associated with strict diagnostic criteria and alterations in HAART therapy regimens.

1641 Patients With Idiopathic IgA Nephropathy: Analysis of the Predictive Value of Urinary Levels of Mannose Binding Lectine (MBL), C4d and C5b-9 To Identify the Presence of Mesangial Deposits of C4d/MBL in Renal Biopsiess

Maria Teresa Salcedo, Alfons Segarra, Irene Sansano, Marta Vidal, Elias Alejandro Jatem, Katheryne Romero, Irene Agraz, Santiago Ramon y Cajal. Vall d´Hebron University Hospital, Barcelona, Spain.

Background: Mesangial C4d deposits in IgA Nephropaty (IgAN) are an independent predictor of poor long-term prognosis. However, due to the focal nature of the deposits, inmunohistochemical and/or inmunofluorescence (IF) studies can lead to false negative results, especially in biopsy samples containing few glomeruli. The aim of this study was to analyze wether the presence of mesangial deposits of C4d and MBL, in patients with IgAN, correlates with urinary levels of MBL, C4d and/or C5b-9, along with clinical, biochemical and histopathological variables, at the time of diagnosis.

Design: This study included 96 patients with idiopathic IgAN, GFR>60 ml/min (CKD-EPI), with a diagnosis of IgAN on renal biopsy (kidney damage evaluation according to Oxford Classification System 2009). The variables collected from each patient were: clinical and anthropometric variables, renal function, proteinuria/creatinine ratio, urine sediment to rule out pyuria or bacteriuria, urine sampling in second morning urine, urinary levels of MBL, C4d and C5b-9 expressed as ratio corrected for proteinuria. Renal biopsy: standard procedures with H/E, PAS, silver and Masson trichromic, IF study: IgA, IgM, IgG and complement, MBL, MASP2, C4d, C5b-9 and C4dbp.

Results: 27 patients (28%) and 69 patients (78%) were classified as C4d positive and C4d negative respectively, on renal biopsy. In the morphological study, patients with mesangial deposits of C4d had increased mesangial (M) and tubulointersticial (T) scores comparing with those without deposits. Urinary levels of C4d, C5b-9 and MBL, adjusted for proteinuria, were significantly higher inC4d+ patients than in C4d- patients. A statistically significant correlation was observed among urinary levels of C5b-9, C4d and MBL. The C4d/proteinuria ratio had a sensitivity of 83% and specificity of 80% for identifying patients with mesangial deposits of C4d/MBL.

Conclusions: 1) the presence of mesangial deposits of C4d, invariably associates with the presence of deposits of MBL, 2) urinary levels of C4d/MBL are useful biomarkers to identify patients with IgA Nephropaty with mesangial C4d deposits on renal biopsy, 3) further studies with several urinary mesurements are required to determine variability, validity and reproducibility of results.

1642 Clinicopathologic Features of Recurrent and De Novo Diabetic Nephropathy in Kidney Transplant Biopsies

Steven Salvatore, Mohamad Alkadi, Sean Campbell, Muthukumar Thangamani, Surya Seshan. Weill Cornell Medical College, New York, NY.

Background: Diabetic nephropathy (DN) is the most common cause of end stage renal disease in the US requiring transplantation. Recurrent or De Novo DN is also common in the transplant setting, playing a role in long-term graft dysfunction.

Design: From 2005-2014, 141 biopsies from 120 transplant patients with DN were studied. DN was classified as 1) donor related if present on biopsy < 1 year from transplant or no diabetes, 2) recurrent if > 1 year with a history of pre-transplant DN, or 3) de novo if > 1yr with post-transplant diabetes. Clinicopathologic parameters were analyzed in 95 patients with adequate clinical history (25 excluded).

Results: Of 95 biopsies, 46 were characterized as recurrent DN, 17 de novo, and 32 donor-related. The recurrent and de novo biopsies were from 63 patients who ranged from 30-81yrs (mean 54.8), had hemoglobin A1c values of 4.1-11.9 (mean 7.5) at time of biopsy, from 40 deceased donor versus 23 living allografts. Rejection was present in 18 patients and other glomerular or tubulointerstitial diseases in 25. The biopsies from longer post-transplant period were associated with a higher creatinine, a higher pathologic DN class, and more vascular disease, but no difference in graft failure, see table 1.

Time (yrs) from transplant biopsy	Recurrent DN				De Novo
	1-3 (mean 2.3)	3-5 (mean 3.9)	5-7 (mean 6.1)	>7 (mean 12.8)	3.5-15 (mean 8)
n	7	15	14	10	17
Type of DM	type 1: 2/7	type 1: 4/15	type 1: 3/14	type 1: 2/10	all type 2
Creatinine (mg/dL)	1.8	2.4	2.4	3.3	2.6
Proteinuria (g/24hr)	3.0	2.1	1.3	1.9	1.5
Class of DN	2a (6), 2b (1)	1 (3), 2a (8), 2b (2), 3 (1), 4 (1)	1 (2), 2a (9), 2b (2), 4 (1)	2a (5), 2b (2), 3 (2), 4 (1)	1 (1), 2a (12), 4 (2)
IF/TA	17%	32%	37%	23%	33%
Vascular Sclerosis (0-3)	1.3	1.8	1.9	1.9	2.3
F/U time (years) from transplant	3.8	5.2	7.3	15.2	10.3
Graft Failure	1/7	1/15	2/14	2/10	3/17

Conclusions: Recurrent or de novo DN may manifest with clinical renal disease or pathological findings as early as 1.5 years following transplantation and should be considered in the differential diagnosis for patients with diabetes and allograft dysfunction. Light, immunofluorescence, and electron microscopy will identify accurately the class and stage of DN, concomitant rejection and other diseases. Earlier detection for at-risk patients may be amenable for appropriate management and help to prevent progression.

1643 Donor-Related Diabetic Nephropathy Predicts Renal Failure in Allograft Biopsies

Steven Salvatore, Mohamad Alkadi, Sean Campbell, Muthukumar Thangamani, Surya Seshan. Weill Cornell Medical College, New York, NY.

Background: Diabetic nephropathy (DN) is the most common cause of end stage renal disease in the US and when present in the transplant setting, may play a role in long-term graft dysfunction. In patients without a history of diabetes, finding features of DN in the immediate for-cause post-transplant biopsy may confer increase risk of allograft dysfunction.

Design: From 2005-2014, 141 biopsies from 120 transplant patients with DN were studied. DN was classified as 1) donor related if present on biopsy < 1 year from transplant or no diabetes, 2) recurrent if > 1 year with a history of pre-transplant DN, or 3) de novo if > 1yr with post-transplant diabetes. Clinicopathologic parameters were analyzed in 95 patients with adequate clinical history (25 excluded).

Results: Of 95 biopsies with features of DN, 46 were characterized as recurrent DN, 17 de novo, and 32 donor-related. Biopsies from transplant kidneys with donor-related DN were done 0.5 years (0 days to 3.6 years) post-transplant and 6 had delayed graft function. Other non-DN related disease was frequently seen, likely prompting biopsy: acute tubular injury (9/32), antibody mediated rejection (3), calcineurin inhibitor toxicity (3), AIN (4), TMA (1) and BKV (1). Pathologic class of DN were as follows: Class 1-3, Class 2a-19, Class 3-10. Class 3 DN lesions are associated with higher level of proteinuria, Cr, and increased vascular sclerosis, see table. Mean follow-up times were 3.8 years for donor-related, 7.5 for recurrent, and 10.3 for de novo. Despite shorter follow-up time, the transplanted kidneys with donor-derived DN had significantly more failure than recurrent DN (53 v 13%, P=.0001) or de novo DN (53 v 18%, P=.016). Recurrent DN and de novo DN had similar rates of graft loss (P=.64).

Class of DN	1	2a	3
n	3	19	10
Creatinine	2.47	4.12	3.88
Proteinuria	0.81	0.83	2.24
IF/TA	23%	29%	23%
Vascular sclerosis (0-3)	1.3	1.8	2.2
F/U time (years) from transplantation	2.1	3.9	4.1
Graft Failure	2/3	9/19	6/10

Conclusions: Despite careful screening of transplant kidney donors, donor related DN may be missed on pre-transplant biopsy and lead to renal dysfunction in the early post-transplant period. Donor related DN is a significant contributor to allograft loss in this population as compared to recurrent or de novo DN. Detection of donor related DN in the transplant predicts poor long term graft survival.

1644 Microarray Gene Expression Profiling Reveals a Direct Relationship Between Matrix Organization and Vascular Development in Renal Allografts

Suman Setty, Heidi Friedeck, Vishal Varma, Michael Walsh, Sanjeev Akkina. University of Illinois at Chicago, Chicago, IL.

Background: Masson trichrome staining assesses the presence and severity of interstitial fibrosis (IF) in renal allografts. However, IF assessment is often complicated by tissue staining artifacts and mild IF is often masked by edema. IF is accompanied by vascular changes such as abnormal capillary proliferation. We propose a surrogate method of assessing IF/chronic graft rejection using a CD31 immunostain. Semi-quantitative analysis of interstitial capillary proliferation and fibrosis was compared with microarray gene expression profiles for genes involved.

Design: Thirty-seven renal allograft biopsies obtained 3-24 months post-transplant, from individuals without infection or rejection, were assessed for abnormal cappillary proliferation using CD31 immunohistochemistry (IHC). A scaled score of interstitial area occupied by abnormal capillaries (ac) of 0-5% received an ac score of 0; 6-25% = ac1, 26-50%= ac2, and more than 50% = ac3. Masson trichrome stains were manually scored, to generate a scaled fibrosis score (ci, following Banff 2005 criteria). The tubulointerstitium was laser capture microdissected from paraffin embedded biopsies and microarray analysis was run using Affimatrix PrimeView gene chip. Gene expression profiles for matrix organization and vascular development were compared to the "ac" scores, to determine a correlation.

Results: Abnormal capillary proliferation in the renal interstitium was proportionally increased along with interstitial fibrosis using the scaled measurements ($r2=0.44, p<0.01$). These scores were compared with microarray analysis of isolated tubulo- interstitium. Numerous pathways were differentially expressed in biopsies with 25% or greater CD31 including those for matrix organization and vascular development. In particular, VEGF-A is differentially expressed between the >25 vs <25% groups of CD31 by IHC, although not all genes from the angiogenesis pathway are upregulated. Pathways involved in RNA processing dominate the highly significant groups.

Conclusions: Fibrosis in the interstitium is a robust indicator of renal graft function with a few exceptions. We observed that abnormal capillary proliferation within the areas of fibrosis can be scored with a similar accuracy as fibrosis. Microarray analysis of the tubulo-interstitium demonstrated significant alterations in expression of molecules involved in matrix organization and vascular development and was able to distinguish between biopsies with >25 vs <25% CD31 levels by IHC. This supports the utility of CD31 IHC as a marker of chronicity in renal allografts.

1645 Urinary Calculi Composition in American Adults in the 21st Century

Aleksandra Sowder, Robert Crosbie, Elisabeth Malmberg, Elizabeth Frank. University of Utah School Health Sciences Center, Salt Lake City, UT; ARUP Institute for Clinical and Experimental Pathology, Salt Lake City, UT.

Background: Urolithiasis is common in the US adult population and incidence appears to be increasing. However, a comprehensive investigation of stone composition has not been performed recently. We sought to assess trends in urolithiasis composition in the US and to reappraise the relationship of age and gender to kidney stone composition in the adult population.

Design: We reviewed composition for all urinary stones submitted to a reference laboratory between January 1, 2009, and December 31, 2013. Specimens were excluded from patient's younger than 18 or older than 99 years of age. Stone composition was determined by Fourier transform infrared spectroscopy (FTIR). Logistic regression analysis was performed to determine associations between stone composition frequency, age, and gender.

Results: A total of 281,997 stones were included in our analysis. Most calculi (85.0%) contained calcium. Almost half (49.6%) of stones were composed of a single element; 47.7% consisted of multiple crystalline components. Calcium oxalate (monohydrate and dihydrate) represented the main component (68.2%) of all stones. Major constituents in the remainder of the calculi analyzed included calcium phosphate (17.8%), uric acid (8.7%), and magnesium ammonium phosphate (MAP, 1.4%).These four constituents accounted for 96.1% of the specimens. Ammonium acid urate, cystine, and calcium carbonate were principal elements in less than 1% of specimens. Although more stones were submitted from males (59.9%) than females (40.1%), calcium oxalate was the most common component in both genders (74.1% M and 59.5% F). However, calcium phosphate stones were more common in females than males (28.5% F, 10.6% M) and uric acid stones more common in males than females (11.0% M, 5.3% F). Stones of all compositions were most prevalent in the sixth decade (ages 51-60 years) for both genders. The incidence of uric acid stones or MAP (infection stones) increased with advancing age. Uric acid and MAP were detected in 2% of calculi analyzed in the 18-31 year old age group and in approximately 23% (uric acid, 18.1%; MAP, 4.8%) of calculi found in the 80 years and older group.

Conclusions: This analysis represents the largest review of urinary stone composition in the US adult population. The results support previously published data that indicate persistence of calcium oxalate as the most common component of urinary calculi, a decreasing incidence of MAP stones and other trends comparable to those noted in a recent European analysis.

1646 Mesangial Cells (MCs) Incubated With Light Chain Deposition Disease (LCDD) But Not Tubulopathic Light Chains (LCs) Switch From Collagen IV To Tenascin Production and Exogenous Metalloproteinase (MMP)-7 Catabolizes Accumulated Tenascin

Jiamin Teng, Chun Zeng, Elba Turbat-Herrera, Guillermo Herrera. Louisiana State University Health Sciences Center, Shreveport, LA.

Background: LCDD is characterized by an increase in mesangial extracellular matrix forming nodules. This process is driven by secretion/activation of transforming growth factor-β by mesangial cells. Normal MCs produce predominantly collagen IV, the main constituent of the mesangial matrix; however, the matrix in the nodules is rich in tenascin with little collagen IV. MMP-7 is involved in the catabolism of tenascin and although activated when MCs are incubated with LCDD-LCs, MMP-7 is not found in the extracellular domain. The mechanisms involved to result in the abnormal matrix are not fully characterized.

Design: MCs are grown on monolayers with 10% FBS RPMI 1640 to 70% confluence, and made quiescent with low serum media for 2 days, then incubated with LCDD and myeloma cast nephropathy (MCN) LCs 10 ug/ml purified from the urine of patients with biopsy-proven LCDD and MCN for 4 days. A single application of MMP-7 5 ng/ml was administered to the MCs in culture incubated with or without LCs. Samples were stained for collagen IV labeled with DyLight 488 (Green) and tenascin labeled with DyLight 593 (red). A Zeiss Axio Observer Z1 inverted microscope with fluorescence capabilities was used to observe findings. Statistical analysis was performed using Zen 2012 SP1 software.

Results: Before the MCs are incubated with LCs, the matrix is entirely composed of collagen IV and when incubated with LCDD-LCs it changed to a tenascin-rich matrix. MCs incubated with MCN-LC do not switch from collagen IV production to tenascin. Once tenascin was noted in the extracellular matrix, exogenous MMP-7 was placed in slide chambers resulting in disappearance of the tenascin.

While MCs by themselves cannot dispose of the tenascin, exogenous MMP-7 catabolized the tenascin that was deposited in the extracellular matrix. These findings, when taken together, indicate that although MCs are capable and indeed increase production of MMP-7 when incubated with LCDD-LCs they are not able to secrete MMP-7 into the extracellular matrix, leading to the matrix accumulation rich in tenascin.

Conclusions: When MCs are incubated with LCDD but not with MCN-LCs there is activation of genes that are normally silent in normal MCs resulting in tenascin production and accumulation. The inability of MCs to secrete MMP-7 into the extracellular matrix is responsible for the buildup of matrix in mesangial nodules. Exogenous MMP-7 destroys accumulated tenascin restoring homeostasis.

1647 Podocyte Loss Precedes Transplant Glomerulopathy in Antibody-Mediated Rejection

Mirna Toukatly, Brent Fall, Behzad Najafian. University of Washington Medical Center, Seattle, WA.

Background: Antibody mediated rejection (AMR) is a major cause of long term kidney allograft loss. Understanding mechanisms of kidney injury due to AMR may lead to novel treatment options. Segmental glomerulosclerosis is commonly found in association with transplant glomerulopathy (TG), suggesting podocyte loss in chronic active AMR (CAMR). We hypothesized that podocyte loss occurs prior to TG.

Design: Urine samples were collected from 22 healthy volunteers and 15 kidney transplant patients, including 11 with AMR (including 4 with acute AMR (AAMR) and 7 with CAMR) and 4 with no AMR (NAMR) (including one with acute cellular rejection and 3 with nonspecific chronic changes). Urine samples from kidney transplant subjects were obtained around the time of biopsies. Biopsy diagnoses were made based on Banff schema in a blind fashion. Urine podocytes were identified on cytospins based on (+) podocalyxin and (–) claudin1 staining, and urine podocytes per gram creatinine (UPC/gCr) was calculated. Percentages of foot process effacement (%FPE) and percentages of foot process detachment from the glomerular basement membranes (%FPD) were estimated on 5 biopsies with TG and 9 biopsies with acute tubular injury (ATI) as controls.

Results: Patients with AMR had prominently more UPC/gCr (3323±3017) than NAMR (662±667; p=0.03) or healthy (1135±960; p=0.003) subjects. However, UPC/gCr was not different between those with AAMR (2662±4125) vs. CAMR (3851±2158). Consistent with this finding, urine albumin creatinine ratio (UACR) was increased in AAMR (p=0.001) and CAMR (p=0.0002) vs. healthy subjects, but was not different in AAMR vs. CAMR. UPC/gCr was directly correlated with UACR (r=0.76, p=0.02) in AMR subjects, but not in healthy subjects. FPD was only observed in biopsies with TG. %FPE, although numerically greater in TG (49±23%) than in ATI (31±24%), was not statistically different between the two groups.

Conclusions: These studies, for the first time, suggest that podocyte loss occurs not only in CAMR, but also during AAMR, and thus, precedes CAMR (TG). Targeting podocyte loss during AMR may improve allograft outcome. Podocyturia may be of prognostic value for long term allograft outcome.

1648 Hic-5 Protects Podocytes From Genotoxic Cell Death By Stabilizing p21

Marcel Tuecking, Jonas Sieber, Peter Mundel, Astrid Weins. Mass General Hospital, Boston, MA; Brigham & Women's Hospital, Boston, MA.

Background: Postmitotic podocytes are an integral part of the glomerular filtration barrier. Podocyte injury and loss are associated with proteinuria, glomerular disease progression and aging. Hic-5, a LIM domain scaffolding protein, is localized at focal adhesions. In immunohistochemical stainings of human biopsies and murine models of proteinuric disease, hic-5 expression is increased in the glomerulus; however, hic-5$^{-/-}$ mice show no kidney phenotype at baseline.

Design: Using an established podocyte cell line *in vitro*, we created hic-5-deficient (hic-5 KD) and non-silencing control shRNA expressing podocytes using a lentiviral-based approach. Q-PCR and Western blots to confirm the efficacy of hic-5 depletion were performed. Cells were exposed to 0.5 µg/ml adriamycin (ADR) to induce DNA damage or 2.5 µM thapsigargin to cause ER stress, and subjected to an annexin V/PI FACS-based cell death assay. Hic-5$^{-/-}$ mice and their WT littermates were challenged by retroorbital injection of 11ug/gBW ADR, and 24h urine protein excretion was measured at baseline, and 2 and 4 weeks post injection. All animals were sacrificed after 4 weeks, and kidneys were examined histologically. Frozen human renal biopsies were stained for hic-5 and the podocyte marker synaptopodin. Images were obtained using a Zeiss ELYRA microscope in structured illumination mode.

Results: Hic-5 KD podocytes showed significantly increased cell death in response to DNA damage after ADR exposure compared to controls. In contrast, there was no difference in cell death following thapsigargin-induced ER stress. Moreover, protein abundance of the known hic-5 target p21 was markedly decreased in hic-5 KD podocytes, while p21 mRNA was increased. Hic-5$^{-/-}$ mice developed 3-fold higher proteinuria 2 weeks post ADR exposure than WT littermates, which correlated closely with a substantially higher incidence of glomerular disease. In humans, a subset of podocytopathies and diabetic nephropathy demonstrated detectable hic-5 in podocytes, while it was only visible in the mesangium of control cases.

Conclusions: Hic-5 has a crucial role in protecting podocytes from genotoxic cell death through stabilization of p21, a critical G1/S transition blocker necessary for efficient DNA repair in postmitotic cells. In the absence of hic-5, G1/S checkpoint control is disabled, and podocytes, impaired in DNA repair and unable to proliferate, undergo cell death, resulting in progressive glomerular damage. Thus, hic-5 may be an attractive drug target in proteinuric kidney disease.

1649 Contribution of Human Smooth Muscle Cells To Vascular AL-(Light Chain Related) Amyloidosis

Moiz Vora, Guillermo Herrera. Louisiana State University Health Sciences Center, Shreveport, LA.

Background: Soluble amyloidogenic light chains can be internalized into a variety of cell types. The endocytosis and processing of amyloidogenic LCs in acquired lysosomes is postulated to be a key step in the formation of amyloid. The vasculature is a common target of amyloidosis wherein amyloid is noted to affect medium to large arterioles with amyloid (Am) deposits in the media and adventitia leading to wall thickening. We hypothesize peripheral vascular smooth muscle cells (VSMCs) contribute to the deposition of amyloid by the uptake and subsequent processing of AL-Am-LCs.

Design: In this study we examine the effects of purified AL-Am- LCs on coronary artery smooth muscle cells in vitro. Human coronary artery smooth muscle cells were plated for culture in Basal Medium. Passage 2 cells [cell density 2 x 10^5 cells/ ml] were subsequently grown to 90% confluency on coverslips placed on 12-well 25 mm plates. Additionally passage 3 cells [cell density 2.6 x 10^5 cells/ml] were grown to 90% confluency on four-chamber plastic slides. These cells were then treated with AL-AM-LC diluted in Basal Medium at a concentration of 10 µg/ml. Cells incubated in culture medium served as control. All cells were incubated at 37^{0}C and 5% CO_2 for 48h, after which the light chains and medium were removed. The cells were fixed in formalin and submitted for H&E, Congo-Red, Thioflavin T, and immunoflorescence for λ light chains.

Results: Cultured smooth muscle cells showed a typical spindle-shaped or polygonal appearance. Amyloid deposits were detected extracellularly when cultured smooth muscle cells were exposed to amyloidogenic light chains. Congo red and thioflavin T stains confirmed the presence of amyloid. Immunoflorescence with lambda light chain revealed extracellular florescent signal co-localized to the foci of amyloid deposition. No amyloid deposits were detected by histochemical techniques in cells incubated with culture medium alone.

Conclusions: Our results support that smooth muscle cells contribute to the pathogenesis of vascular amyloidosis and provide a platform to further investigate the role of vascular smooth muscle cells in the production of AL-amyloid.

1650 Putting It All Together in the Renal Biopsy: Software Analysis of Sequential Whole Slide Images With Three Dimensional Volume Rendering

Ashley Ward, Devin Rosen, Zsuzsanna Zsengeller, C Law, Seymour Rosen, Beverly Faulkner-Jones. Beth Israel Deaconess Medical Center, Boston, MA; Kitware, Inc., Clifton Park, NY.

Background: Analyzing multiple serial tissue sections is a laborious task. Recently we presented software tools for aligning whole slide images of serial tissue sections with different colorimetric parameters (USCAP abstract, 2013). The integration and understanding of these multiple parameters in serial sections of human renal biopsies can provide insights into renal injury.

Design: We now show how this sequential analysis can be applied to renal biopsy material using basement membrane stains (PAS, silver methenamine), vascular markers (CD34; smooth muscle heavy chain myosin), epithelial markers (AE1/AE3; CAM5.2) and mitochondrial immunostains (cytochrome oxidase 1and 4). This methodology can be used to define three-dimensional constructs.

Results: Sequential sections from a renal biopsy were aligned using this software. There was considerable, but evidently localized calcium oxalate deposition related to a gastric bypass procedure. Using sequential analysis, it was apparent that the crystals localized to tubules causing reactive epithelial changes.The associated interstitial tissues were fibrotic with obliteration of the capillary network. The mitochondrial content of the involved cellular elements could be defined. Furthermore, a 3-dimensional construct of the calcium oxalate crystalline mass was generated.

Figure 1. Aligned serial sections of renal biopsy, 16 sections represented, total 70 (left). H&E with evident calcium oxalate crystal deposition; section polarized (mid). 3-dimensional construct of crystals (right).

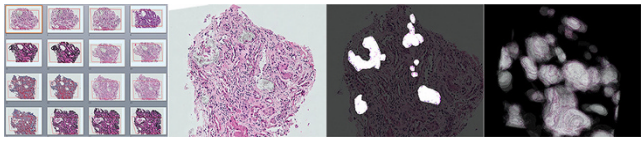

Conclusions: The integrated sequential analysis of serial sections allows analyses of consecutive image data sets, allowing a rapid and simplified study of multiple parameters. Three-dimensional images can also be constructed and do allow better appreciation of vascular networks, tubular structures and glomeruli. In this instance, the extent of crystal deposition was only really understood by the 3-dimensional study.

1651 Macrophage Thymosin β4 Knockdown Alone Is Insufficient To Modulate Kidney Macrophage Infiltration and Interstitial Fibrosis

Jaewon Yang, Sebastian Potthoff, Yiqin Zuo, Hai-chun Yang, Agnes Fogo. Vanderbilt University, Nashville, TN.

Background: We previously found thymosin β4 (Tβ4) increased kidney interstitial fibrosis in early stage of unilateral ureteral obstruction (UUO), and its degradation product, Ac-SDKP, reduced fibrosis with decreased macrophage infiltration. The effects were not observed in PAI$^{-/-}$ with UUO, suggesting PAI-1 dependence. Further, knockdown of Tβ4 in macrophages induced more M2 polarization in vitro. β6$^{-/-}$ mice are incapable of integrin avβ6-dependent TGF-b1 activation and resistant to fibrosis after UUO. Additional AngII induced fibrosis in β6$^{-/-}$ UUO mice, with increased PAI-1 and macrophage infiltration. We now investigated whether modulation of Tβ4 impacts interstitial fibrosis by regulating macrophage infiltration in UUO and β6$^{-/-}$ UUO+AngII mice.

Design: Tβ4 short hairpin RNA floxed mice were crossed with lysM-Cre mice to generate macrophage-specific Tβ4 knockdown mice. Tβ4 shRNA$^+$/LysMCre$^-$ and Tβ4 shRNA$^+$/LysMCre$^+$ mice underwent UUO with sacrifice at D7. Next, β6$^{-/-}$ mice underwent UUO and AngII infusion, with sacrifice at D5. Mice were treated with or without additional Tβ4 and POP-inhibitor (an inhibitor of Tβ4 degradation).

Results: Tβ4 knockdown in macrophages was confirmed in isolated peritoneal thioglycolate-elicited macrophages from Tβ4 shRNA$^+$/LysMCre$^+$ mice. On D7 after, macrophage infiltration (F4/80$^+$ cells) was similarly increased in Tβ4 shRNA$^+$/LysMCre$^+$ (43.2±3.4/HPF) and Tβ4 shRNA$^+$/LysMCre$^-$ mice (41.1±4.1/HPF). Interstitial fibrosis was also similar (Tβ4 shRNA$^+$/LysMCre$^+$ 0.54±0.13 *vs.* Tβ4 shRNA$^+$/LysMCre$^-$ 0.59±0.13%, pNS). In the β6$^{-/-}$ UUO+AngII model, kidney Tβ4 expression was significantly increased by adding Tβ4 and POP-inhibitor. Collagen III mRNA was significantly increased, but total collagen protein was not changed by Tβ4 and POP-inhibitor treatment. Treatment did not further increase macrophage infiltration (Tβ4 9.7±1.6, *vs.* AngII+UUO 10.7±1.4/HPF, pNS).

Conclusions: We conclude that reduced Tβ4 only in macrophages is not sufficient to modulate fibrosis in UUO mice with intact PAI-1 and TGFβ pathways. We also confirm that adding AngII restores fibrosis in β6$^{-/-}$ UUO mice, with associated high PAI-1 but no TGFβ activation. Increasing Tβ4 further in this model does not enhance fibrosis, supporting that either Tβ4 is already maximally induced or Tβ4 effects are in part dependent on intact TGFβ activation.

1652 Restoring Glomerular VEGF Expression Stimulates Glomerular Capillary Growth in 5/6 Nx Mice

Ya-fen Yu, Ying Wu, Hai-chun Yang, Agnes Fogo. Wuxi Fouth Hospital, Jiangnan University, Wuxi, Jiangsu, China; Children's Hospital, Jiaotong University, Shanghai, China; Vanderbilt University, Nashville, TN.

Background: Glomerulosclerosis is characterized by increased matrix and obliteration of capillary lumens. VEGF, a pro-angiogenesis factor, is derived from podocytes and is therefore decreased in sclerotic glomeruli. We previous found that VEGF stimulates glomerular endothelial cell expression of DLL4, a marker for endothelial tip cell. High dose angiotensin II receptor blocker (ARB) induces glomerulosclerosis regression in part by decreasing matrix accumulation. In this study, we investigated whether the phenotype of regression of sclerotic glomeruli is affected by combination of restoring VEGF and ARB.

Design: Subtotal nephrectomy (5/6Nx) was performed in podocin-rtTA/TRE-human VEGF (RV) and podocin-rtTA mice (R). All mice underwent renal biopsy at week 8 and were sacrificed four weeks later. Mice were divided into four groups with equal average glomerulosclerosis index (SI, 0-4 scale) at biopsy: R group (n=11), RV group (n=10), R+ARB group (n=12), RV+ ARB group (n=9). From week 8 until 12, doxycycline was added in drinking water to induce VEGF specifically in podocytes.

Results: By week 12, total glomerular VEGF level was reduced to 20.5% and 30.3% of normal level in R and R+ARB, respectively, and restored to 65.8% and 78.1% in RV and RV+ARB. Glomerular volume was not different among groups at week 8 and 12. ARB and RV+ARB significantly reduced collagen IV staining in glomeruli (31.11±2.05 and 28.20±1.05%, respectively) *vs.* R (37.50±1.55%). Capillary number

increased 77.6% and 144.6% in RV and RV+ARB, while there were no change in R and R+ARB. Capillary length increased 18.5% in RV and 57.8% in RV+ARB, compared to 23.8% in R and 36.7% in R+ARB.
Conclusions: We conclude that ARB reduces glomerular matrix accumulation, and restoring VEGF in sclerotic glomeruli induces more new capillary branches, both of which contribute to ameliorate glomerulosclerosis.

1653 Histopathologic Evidence of Contrast-Induced Nephropathy

Cynthia Zhao, Luyu Yao, Wayne Zhang, Xin Gu. Louisiana State University Health Sciences Center, Shreveport, LA.
Background: Contrast-induced nephropathy (CIN) is the third leading cause of acute renal failure in hospitalized patients. The mechanisms of CIN are not well understood. Direct renal tubular cell damage is hypothesized as one of the major causes. However, there is limited histopathologic evidence supporting it. Proximal tubules are very vulnerable to renal toxic medications or chemicals. We hypothesize that CIN may result from direct structural damage of proximal tubules caused by contrast media (CM). The objective of this study is to investigate the histomorphologic changes of CIN.
Design: Our CIN mouse model is created by inhibiting prostaglandin and nitric oxide syntheses followed by administration of Iodixanol, one of the most commonly used CM. This model mimics the clinical CIN scenario because the hospitalized patients likely have underlining renal dysfunction with low prostaglandin and nitric oxide levels. Two dosages of Iodixanol, 6.24 gI/kg and 12.48 gI/kg, were given based on body weight. C57B1/6J mice received indomethacin (a prostaglandin synthesis inhibitor, 10 mg/kg) and Nω-Nitro-L-arginine methyl ester (L-NAME, a nitric oxide synthase inhibitor, 10mg/kg) intraperitoneally before injection of Iodixanol. The mice in control group received indomethacin and L-NAME followed by normal saline instead of Iodixanol. Kidneys were harvested after 24 hours. The specimens were fixed with 10% formalin, embedded in paraffin, and stained with Hematoxylin and Eosin (H&E) and Periodic Acid-Schiff (PAS) for histopathologic evaluation.
Results: The histopathologic changes were mainly identified in the proximal tubular epithelial cells. The glomeruli and medullary areas showed no significant abnormalities. The kidney in low dose group revealed mild acute tubular injury manifested with cellular edema and prominent vacuolar degeneration. The kidney in high dose group presented with moderate acute tubular injury with extensive cellular edema and prominent vacuolar degeneration. The PAS stain in high dose group also showed segmental brush border loss of the tubular epithelial cells. The control group revealed no significant tubular injury.
Conclusions: Our data showed clear histopathologic evidence of renal proximal tubular epithelial cell injury caused by CM with dosage-dependent severity. There were no significant medullary changes. Direct toxicity-related renal tubular cell damage is likely to be one of the mechanisms of CIN. Further investigation of protective agents against CIN is planned.

Liver

1654 Nuclear Forkhead Box O3a Expression in Hepatocellular Carcinoma: Correlation With Clinicopathologic Features and Survival

Hyein Ahn, Jongmin Sim, Hyunsung Kim, Kijong Yi, Yumin Chung, Abdul Rehman, Seung Sam Paik, Dong Ho Choi, Kiseok Jang. Hanyang University Hospital, Seoul, Republic of Korea.
Background: Forkhead box O3a (FoxO3a) is a transcription factor belonging to the subfamily of winged-helix forkhead box family which plays a critical role in the regulation of a wide spectrum of biological processes. FoxO3a is known as a tumor suppressor that regulates a variety of proapoptotic genes, and inactivates the PI3k-Akt oncogenic pathway. A recent study has demonstrated that FoxO3a with nuclear β-catenin promotes the survival of cancer cells, tumor expansion, and metastasis.
Design: A total of 223 cases of hepatocellular carcinoma (HCC) with adequate paraffin-embedded tissue samples were collected and reviewed. Expression of FoxO3a, β-catenin, and Ki-67 was analyzed by immunohistochemical staining on tissue microarrays. We evaluated the relation between FoxO3a overexpression and various clinicopathologic features. In addition, we investigated the correlations between FoxO3a overexpression and expression of β-catenin and Ki-67.
Results: The nuclear FoxO3a overexpression was correlated with aggressive phenotypes of HCC, such as advanced AJCC stage ($p = 0.002$), vascular invasion ($p < 0.001$), and higher histologic grade ($p < 0.001$). The Kaplan-Meier survival curves revealed that FoxO3a overexpression was significantly associated with poor disease free survival ($p = 0.042$, log-rank test). FoxO3a overexpression was associated with higher Ki-67 labeling index ($p < 0.001$).
Conclusions: Our results demonstrate that FoxO3a overexpression is associated with poor prognostic factor in HCC, and correlates with higher Ki-67 labeling index. These controversial findings should be clarified with further investigation, which can provide opportunities for the development of biomarker or potential targeted therapy.

1655 Cystadenomas of the Liver and Extrahepatic Bile Ducts. Morphologic and Immunohistochemical Characterization of the Biliary and Intestinal Variants

Jorge Albores-Saavedra, Juan Cordova-Ramon, Fredy Chable-Montero, Rita Dorantes-Heredia, Donald Henson. Medica Sur Clinic and Foundation, Mexico, DF, Mexico; Instituto Nacional de Ciencias Médicas y Nutrición "Salvador Zubirán", Mexico, DF, Mexico; Uniformed Services University of the Health Sciences, Bethesda, MD.
Background: Cystadenomas of the liver and extrahepatic bile ducts (EHBD) are uncommon neoplasms whose terminology and epithelial phenotype has been a source of controversy. The generic term "mucinous cystic neoplasm" has been recommended by the World Health Organization (WHO).
Design: We identified 20 cystadenomas of which 16 originated in the liver and 4 in the EHBD. Clinical and follow-up information were obtained from the medical records. Gross findings were obtained from the surgical pathology reports. The percentage of the epithelial lining cells: biliary, intestinal and foveolar, was estimated for each tumor. Multiple H&E stained sections were available for review in all 20 cases. From selected paraffin blocks additional slides were prepared for immunohistochemical analysis.
Results: Eighteen patients were women, with a mean age of 36.5 years. The tumor size ranged from 4 to 29 cm (average 11 cm). The cyst fluid in 13 tumors was described as serous, in two as clear, in two others as hemorrhagic, and in one as serous and mucinous. Only in 2 tumors was the fluid described as mucinous. In 18 cystadenomas the predominant epithelial lining consisted of a single layer of cuboidal or low-columnar non-dysplastic cells similar to those of the gallbladder and bile ducts. These cells expressed cytokeratin (CK) 7 and 19, and focally MUC1. Only two cystadenomas showed predominant intestinal differentiation characterized by mature goblet cells and columnar absorptive cells. These cells expressed CDX2, MUC2 and CK20. These 2 tumors showed areas of high-grade dysplasia and invasive adenocarcinoma with intestinal phenotype. A subepithelial ovarian-like stroma was present in all tumors. None of the patients died as a result of the tumors.
Conclusions: Our findings indicate that there are two types of cystadenomas in the liver and EHBD. The most common (80%), lined predominantly by non-dysplastic biliary epithelium appears to lack malignant potential, and the second showing predominantly intestinal differentiation, may progress to high-grade dysplasia and invasive adenocarcinoma. We believe that the term "mucinous cystic tumor" recommended by the WHO for all cystadenomas of the liver and EHBD is a misnomer.

1656 Autoimmune Hepatitis: Review of Validity of Histologic Features Included in the Simplified Criteria Proposed By the International Autoimmune Hepatitis Group (IAIHG)

Dana Balitzer, Nafis Shafizadeh, Najeeb Alshak, Sanjay Kakar. University of California, San Francisco, CA; Kaiser Permanente, Los Angeles, CA.
Background: Histologic features, autoantibodies, serum IgG and negative viral serology are part of Simplified Criteria adopted by IAIHG, which regard diagnosis of autoimmune hepatitis(AIH) as definite(≥7 points) or probable(6 points). Histologic features in these criteria are(1)interface hepatitis with portal lymphocytic/lymphoplasmacytic cells extending into lobule (2)emperipolesis (3)rosettes. Presence of all 3 features is typical of AIH(2 points), while a chronic hepatitis picture without all 3 features is compatible with AIH(1 point). The validity of these histologic features for AIH has not been examined.
Design: Clinical data and liver biopsies were reviewed for 89 AIH, 23 primary biliary cirrhosis(PBC) and 5 non-AIH acute hepatitis. The Simplified Criteria score was calculated.Copper and CK7 stains were done in 66 cases.
Results: Emperipolesis and rosettes were seen in 78% and 39% AIH, and 16% and 61% of non-AIH cases. Both features were present in 26% AIH and 17% non-AIH. Copper and CK7 stains were positive in 20% and 43% AIH, all of which had at least bridging fibrosis. Using features of Simplified Criteria, 26% AIH received 2 histologic points(typical AIH), and 60% received 1 histologic point(compatible with AIH). Using our proposed histologic features, 80% and 11% AIH received 2 and 1 histologic points. The proposed histologic features led to increase in Simplified Criteria score of AIH cases from 6(probable AIH) to 7(definite AIH) in 8%, and 5(no AIH) to 6(probable AIH) in 10% cases. There was no increase in score in PBC or non-AIH acute hepatitis.

Histologic Score	Proposed histologic Features
1	Hepatitis with mild or moderate necroinflammatory activity (at least Ishak A2, B1, and/orC2).
2	Any one of the following additional features: (a)Plasma cells: numerous or in clusters (b)CK7 and copper stains negative (for chronic cases with Ishak fibrosis score 3, not applicable toacute cases) (c)High necroinflammatory activity (Ishak >A3, B2 and/or C3).

Conclusions: The requirement of rosettes and emperipolesis in Simplified Criteria leads to a low histologic score even in typical AIH. These features are not specific for AIH and are present in a few PBC and majority of non-AIH acute hepatitis. We propose new histologic features that increase histologic and total scores in AIH, leading to increase in sensitivity of Simplified Criteria for diagnosis of AIH without misclassification of PBC or non-AIH hepatitis cases.